Engineering and Probing Topological Bloch Bands in Optical Lattices

Monika Aidelsburger, Marcos Atala, Michael Lohse, Christian Schweizer, Julio Barreiro

Christian Gross, Stefan Kuhr, Manuel Endres, Marc Cheneau,
Takeshi Fukuhara, Peter Schauss, Sebastian Hild, Johannes Zeiher

Ulrich Schneider, Simon Braun, Philipp Ronzheimer,
Michael Schreiber, Tim Rom, Sean Hodgman

Ulrich Schneider, Monika Schleier-Smith, Lucia Duca, Tracy Li, Martin Reitter,
Josselin Bernadoff, Henrik Lüschen

Ahmed Omran, Martin Boll, Timon Hilker, Michael Lohse,
Thomas Reimann, Alexander Keesling, Christian Gross

Simon Fölling, Francesco Scazza, Christian Hofrichter,
Pieter de Groot, Moritz Höfer

Christoph Gohle, Tobias Schneider, Nikolaus Buchheim, Zhenkai Lu

Humboldt Research Awardees:
N. Cooper, C. Salomon, W. Ketterle

Max-Planck-Institut für Quantenoptik
Ludwig-Maximilians Universität

funding by
€ MPG, European Union, DFG
$ DARPA (OLE)

erc synergy

www.quantum-munich.de

Sunday 22 June 14

Sunday 22 June 14

Outline

Realizing Artificial Gauge Fields

1. Realizing the Hoftstadter & Quantum Spin Hall Hamiltonian
2. 'Meissner'-currents in bosonic flux ladders

Outline

Realizing Artificial Gauge Fields

1. Realizing the Hoftstadter & Quantum Spin Hall Hamiltonian
2. 'Meissner'-currents in bosonic flux ladders

Probing Topological Features of Bloch Bands

3. Probing Zak Phases in Topological Bands
4. An 'Aharonov Bohm' Interferometer for measuring Berry curvature

Realizing Artificial Gauge Fields in Optical Lattices

Quantum Hall Effect in 2D Electron Gases

Integer Quantum Hall Effect

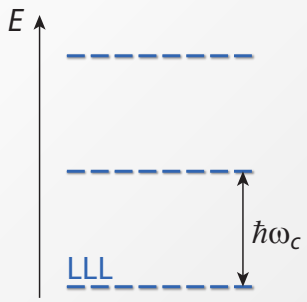

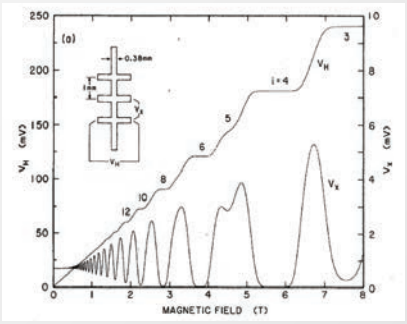

$$\sigma_{xy} = \nu e^2/h$$

ν Integer

Chern Insulators
(w/o magnetic field
see D. Haldane 1988)

Fractional Quantum Hall Effect

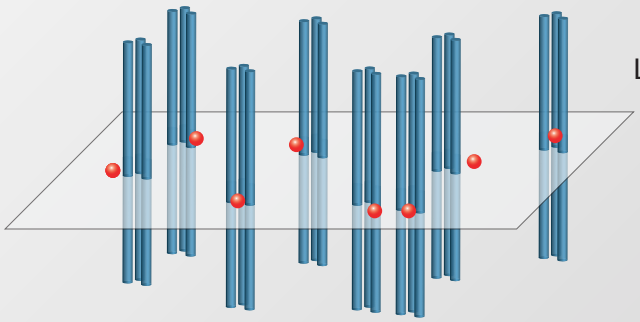

Laughlin state at $\nu = 1/3$

flux quantum $\phi_0 = h/ec$

electron

State of the Art

1) Rotation

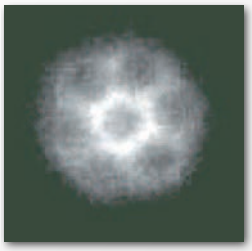

In rapidly rotating gases, ***Coriolis force*** is equivalent to ***Lorentz force***.

$$\mathbf{F}_{\mathrm{L}} = q\,\mathbf{v}\times\mathbf{B} \quad \Longleftrightarrow \quad \mathbf{F}_{\mathrm{C}} = 2m\,\mathbf{v}\times\Omega_{\mathrm{rot}}$$

K. Madison *et al.*, PRL (2000)
J.R. Abo-Shaeer *et al.* Science (2001)

2) Raman Induced Gauge Fields

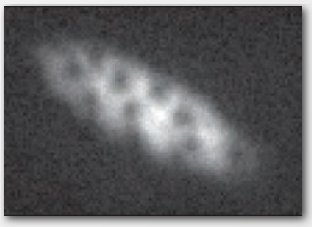

Spatially dependent optical couplings lead to a **Berry phase** analoguous to the **Aharonov-Bohm phase**

Y. Lin *et al.*, Nature (2009)

Gauge Fields

State of the Art

1) Rotation

In rapidly rotating gases, ***Coriolis force*** is equivalent to ***Lorentz force***.

$\mathbf{v}\times\Omega_{\mathrm{rot}}$

t al., PRL (2000)
. Science (2001)

Problem in both cases: small B-fields (large ν>1000 for now), heating...

2) Raman

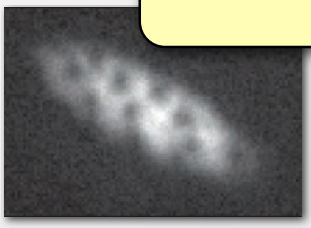

Spatially dependent optical couplings lead to a **Berry phase** analoguous to the **Aharonov-Bohm phase**

Y. Lin *et al.*, Nature (2009)

Artificial B-Fields with Ultracold Atoms

Controlling atom tunneling along *x* with Raman lasers leads to effective tunnel coupling with spatially-dependent Peierls phase $\varphi(\mathbf{R})$

$$\hat{H} = -\sum_{\mathbf{R}} \left(K e^{i\varphi(\mathbf{R})} \hat{a}^{\dagger}_{\mathbf{R}} \hat{a}_{\mathbf{R}+\mathbf{d}_x} + J \hat{a}^{\dagger}_{\mathbf{R}} \hat{a}_{\mathbf{R}+\mathbf{d}_y} \right) + \text{h.c.}$$

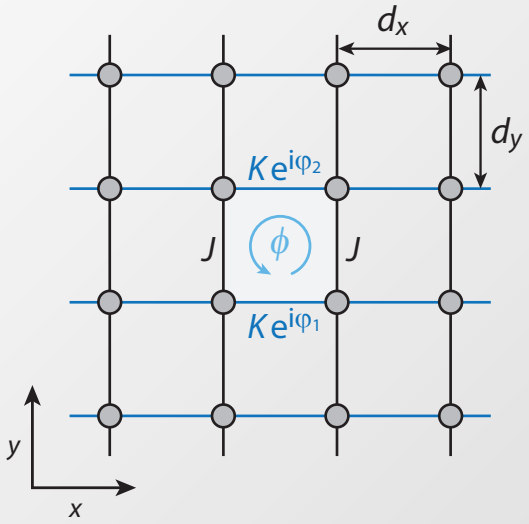

Magnetic flux through a plaquette:

$$\phi = \int_{\square} B \, \mathrm{d}S = \varphi_1 - \varphi_2$$

D. Jaksch & P. Zoller, New J. Phys. (2003)
F. Gerbier & J. Dalibard, New J. Phys. (2010)
N. Cooper, PRL (2011)
E. Mueller, Phys. Rev. A (2004)
L.-K. Lim et al. Phys. Rev.A (2010)
A. Kolovsky, Europhys. Lett. (2011)

see also: lattice shaking
E.Arimondo, PRL(2007) , K. Sengstock, Science (2011),
M. Rechtsman & M. Segev, Nature (2013)

Gauge Fields

Artificial B-Fields with Ultracold Atoms

Controlling atom tunneling along *x* with Raman lasers leads to effective tunnel coupling with spatially-dependent Peierls phase $\varphi(\mathbf{R})$

$$\hat{H} = -\sum_{\mathbf{R}} \left(K e^{i\varphi(\mathbf{R})} \hat{a}^{\dagger}_{\mathbf{R}} \hat{a}_{\mathbf{R}+\mathbf{d}_x} + J \hat{a}^{\dagger}_{\mathbf{R}} \hat{a}_{\mathbf{R}+\mathbf{d}_y} \right) + \text{h.c.}$$

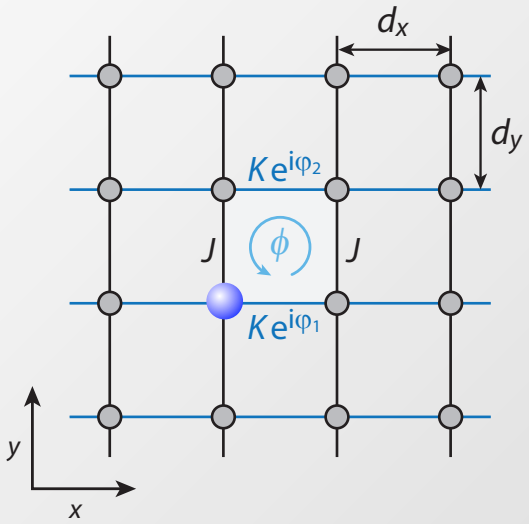

Magnetic flux through a plaquette:

$$\phi = \int_{\square} B \, \mathrm{d}S = \varphi_1 - \varphi_2$$

D. Jaksch & P. Zoller, New J. Phys. (2003)
F. Gerbier & J. Dalibard, New J. Phys. (2010)
N. Cooper, PRL (2011)
E. Mueller, Phys. Rev. A (2004)
L.-K. Lim et al. Phys. Rev.A (2010)
A. Kolovsky, Europhys. Lett. (2011)

see also: lattice shaking
E.Arimondo, PRL(2007) , K. Sengstock, Science (2011),
M. Rechtsman & M. Segev, Nature (2013)

Sunday 22 June 14

Artificial B-Fields with Ultracold Atoms

Controlling atom tunneling along *x* with Raman lasers leads to effective tunnel coupling with spatially-dependent Peierls phase $\varphi(\mathbf{R})$

$$\hat{H} = -\sum_{\mathbf{R}} \left(K e^{i\varphi(\mathbf{R})} \hat{a}^{\dagger}_{\mathbf{R}} \hat{a}_{\mathbf{R}+\mathbf{d}_x} + J \hat{a}^{\dagger}_{\mathbf{R}} \hat{a}_{\mathbf{R}+\mathbf{d}_y} \right) + \text{h.c.}$$

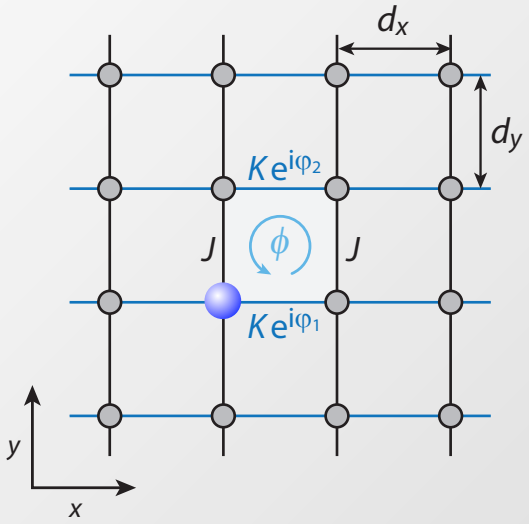

Magnetic flux through a plaquette:

$$\phi = \int_{\square} B \, \mathrm{d}S = \varphi_1 - \varphi_2$$

D. Jaksch & P. Zoller, New J. Phys. (2003)
F. Gerbier & J. Dalibard, New J. Phys. (2010)
N. Cooper, PRL (2011)
E. Mueller, Phys. Rev. A (2004)
L.-K. Lim et al. Phys. Rev.A (2010)
A. Kolovsky, Europhys. Lett. (2011)

see also: lattice shaking
E.Arimondo, PRL(2007) , K. Sengstock, Science (2011),
M. Rechtsman & M. Segev, Nature (2013)

Gauge Fields

Artificial B-Fields with Ultracold Atoms

Controlling atom tunneling along *x* with Raman lasers leads to effective tunnel coupling with spatially-dependent Peierls phase $\varphi(\mathbf{R})$

Fluxes corresponding to severals thousand Tesla magnetic field strength are possible!

D. Jaksch & P. Zoller, New J. Phys. (2003)
F. Gerbier & J. Dalibard, New J. Phys. (2010)
N. Cooper, PRL (2011)
E. Mueller, Phys. Rev. A (2004)
L.-K. Lim et al. Phys. Rev.A (2010)
A. Kolovsky, Europhys. Lett. (2011)

see also: lattice shaking
E.Arimondo, PRL(2007) , K. Sengstock, Science (2011),
M. Rechtsman & M. Segev, Nature (2013)

Sunday 22 June 14

Harper Hamiltonian and Hofstadter Butterfly

Harper Hamiltonian: J=K and ϕ uniform.

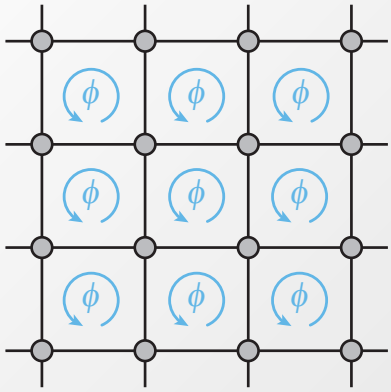

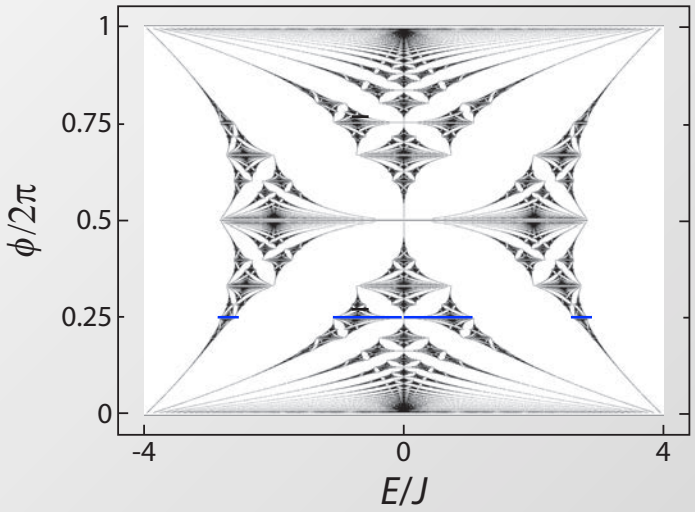

The lowest band is topologically equivalent to the lowest Landau level.

D.R. Hofstadter, Phys. Rev. B**14**, 2239 (1976)
see alo Y. Avron, D. Osadchy, R. Seiler, Physics Today 38, 2003

Experimental method

- Atoms in a 2D lattice
- Tunneling inhibited along one direction using energy offsets

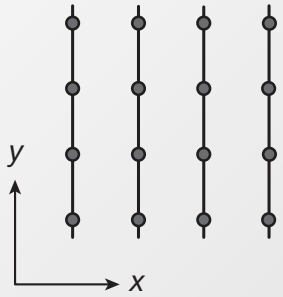

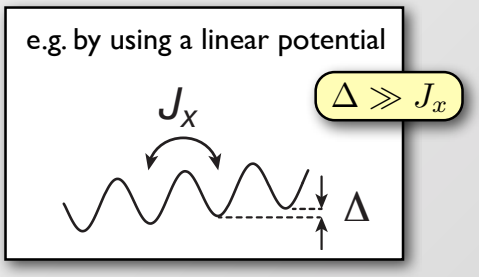

M. Aidelsburger *et al.*, PRL (2011); M. Aidelsburger *et al.*, Appl. Phys. B (2013)

Experimental method

- Atoms in a 2D lattice
- Tunneling inhibited along one direction using energy offsets

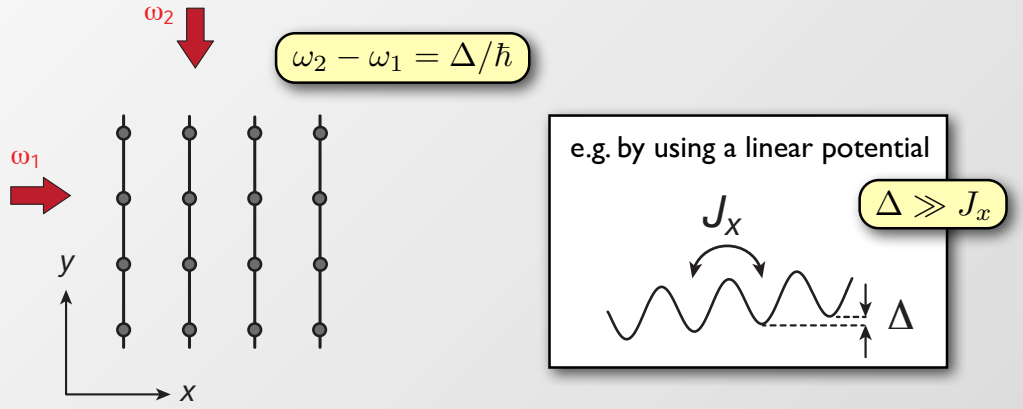

- Induce resonant tunneling with a pair of ***far-detuned*** running-wave beams
  → ***Reduced heating*** due to spontaneous emission compared to Raman-assisted tunneling!
  → ***Independent*** of the internal structure of the atom

M. Aidelsburger *et al.*, PRL (2011); M. Aidelsburger *et al.*, Appl. Phys. B (2013)

Experimental method

- Interference creates a running-wave that ***modulates*** the lattice
- The ***phase of the modulation*** depends on the position in the lattice

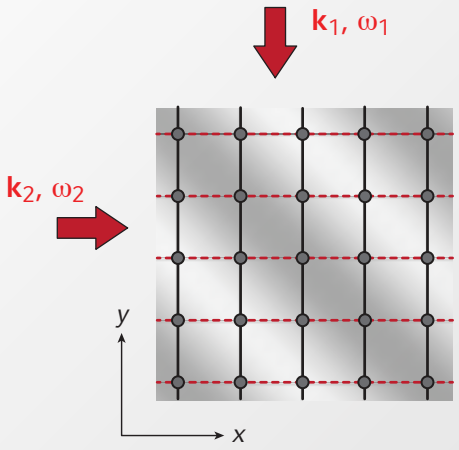

Lattice modulation:

$$V_K^0 \cos(\omega t + \phi(\mathbf{r}))$$

with ***spatial-dependent*** phase

$$\phi(\mathbf{r}) = \delta\mathbf{k} \cdot \mathbf{r}$$

$$\delta\mathbf{k} = \mathbf{k}_2 - \mathbf{k}_1$$
$$\omega = \omega_2 - \omega_1$$

- Realization of ***time-dependent*** Hamiltonian, where tunneling is restored
- Discretization of the phase due to underlying lattice → $\phi_{m,n}$

M. Aidelsburger *et al.*, PRL (2011); M. Aidelsburger *et al.*, Appl. Phys. B (2013)

Experimental method

- Time-dependent Hamiltonian:

$$\hat{H}(t) = \sum_{m,n} \left(-J_x \ \hat{a}^\dagger_{m+1,n} \hat{a}_{m,n} - J_y \ \hat{a}^\dagger_{m,n+1} \hat{a}_{m,n} + \text{h.c.} \right)$$

$$+ \sum_{m,n} \left[m\Delta + V_K^0 \cos(\omega t + \phi_{m,n}) \right] \hat{n}_{m,n}$$

Artificial magnetic fields

Experimental method

- Time-dependent Hamiltonian:

$$\hat{H}(t) = \sum_{m,n} \left(-J_x \ \hat{a}^\dagger_{m+1,n} \hat{a}_{m,n} - J_y \ \hat{a}^\dagger_{m,n+1} \hat{a}_{m,n} + \text{h.c.} \right)$$

$$+ \sum_{m,n} \left[m\Delta + V_K^0 \cos(\omega t + \phi_{m,n}) \right] \hat{n}_{m,n}$$

- Can be mapped on an effective time-averaged time-independent Hamiltonian for $\hbar\omega \gg J_x, J_y, U$

$$\hat{H}_{eff} = \sum_{m,n} \left(-K e^{i\phi_{m,n}} \ \hat{a}^\dagger_{m+1,n} \hat{a}_{m,n} - J \ \hat{a}^\dagger_{m,n+1} \hat{a}_{m,n} + \text{h.c.} \right)$$

- To avoid excitations to higher bands $\hbar\omega$ has to be smaller than the band gap

F. Grossmann and P. Hänggi, EPL (1992)
M. Holthaus, PRL (1992)
A. Kolovsky, EPL (2011); A. Eckardt, PRL (2005)
A. Eckhardt, EPL (2007); P. Hauke, PRL (2012)
A. Bermudez, PRL (2011); A. Bermudez, NJP (2012)

Experimental method

- Time-dependent Hamiltonian:

$$\hat{H}(t) = \sum_{m,n} \left(-J_x \ \hat{a}^\dagger_{m+1,n} \hat{a}_{m,n} - J_y \ \hat{a}^\dagger_{m,n+1} \hat{a}_{m,n} + \text{h.c.} \right)$$

$$+ \sum_{m,n} \left[m\Delta + V_K^0 \cos(\omega t + \phi_{m,n}) \right] \hat{n}_{m,n}$$

- Can be mapped on an e…nian for $\hbar\omega \gg J_x, J_y, U$

Note: Corrections could be important!
see e.g. N. Goldman & J. Dalibard arXiv:1404.4373
& related work A. Polkovnikov

$$\hat{H}_{eff} = \sum_{m,n} \left(-K e^{i\phi_{m,n}} \ \hat{a}^\dagger_{m+1,n} \hat{a}_{m,n} - J \ \hat{a}^\dagger_{m,n+1} \hat{a}_{m,n} + \text{h.c.} \right)$$

- To avoid excitations to higher bands $\hbar\omega$ has to be smaller than the band gap

F. Grossmann and P. Hänggi, EPL (1992)
M. Holthaus, PRL (1992)
A. Kolovsky, EPL (2011); A. Eckardt, PRL (2005)
A. Eckhardt, EPL (2007); P. Hauke, PRL (2012)
A. Bermudez, PRL (2011); A. Bermudez, NJP (2012)

Effective coupling strength

Effective coupling strength:

$$K = J_x \mathcal{J}_1(x)$$
$$J = J_y \mathcal{J}_0(x)$$

$\mathcal{J}_\nu(x)$: Bessel-functions of the first kind

and $x = \dfrac{f(\eta) V_K^0}{\Delta}$

η : Phase difference of the modulation between neighboring bonds

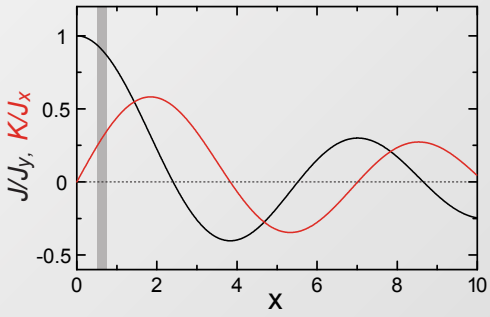

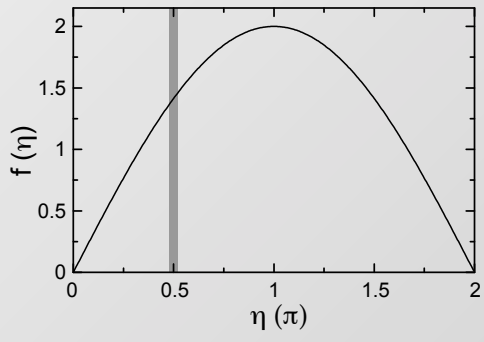

see also: H. Lignier et al. PRL (2007)

Experimental setup

Experimental parameters:

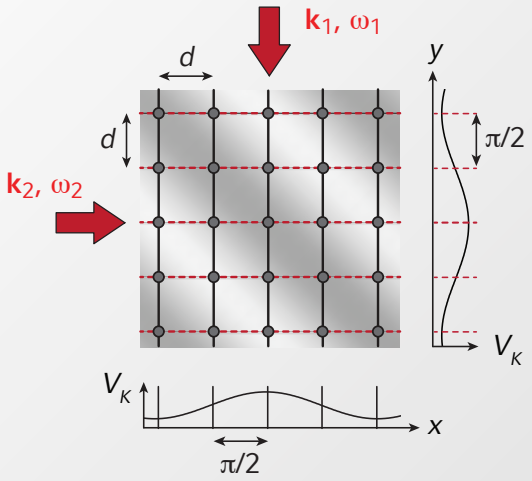

$$|\mathbf{k}_1| \simeq |\mathbf{k}_2| = \frac{\pi}{2d}$$

$$\Rightarrow \phi_{m,n} = \frac{\pi}{2}(m+n)$$

Artificial magnetic fields

Experimental setup

Experimental parameters:

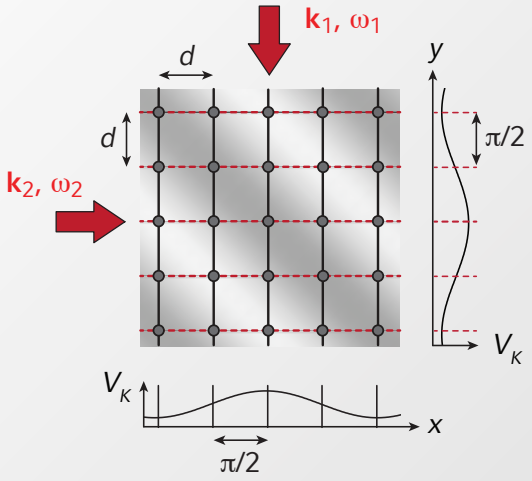

$$|\mathbf{k}_1| \simeq |\mathbf{k}_2| = \frac{\pi}{2d}$$

$$\Rightarrow \phi_{m,n} = \frac{\pi}{2}(m+n)$$

Flux through one unit cell:

$$\Phi = \phi_{m,n+1} - \phi_{m,n} = \frac{\pi}{2}$$

depends only on phase difference along y!

Experimental setup

Experimental parameters:

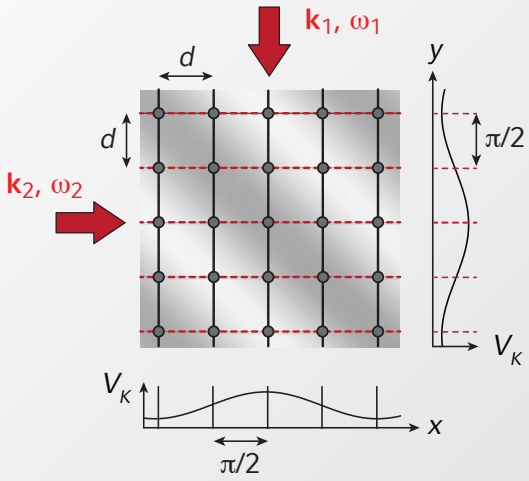

$$|\mathbf{k}_1| \simeq |\mathbf{k}_2| = \frac{\pi}{2d}$$

$$\Rightarrow \phi_{m,n} = \frac{\pi}{2}(m+n)$$

Flux through one unit cell:

$$\Phi = \phi_{m,n+1} - \phi_{m,n} = \frac{\pi}{2}$$

depends only on phase difference along y!

The value of the flux is ***fully tunable*** by changing the geometry of the driving-beams!

Laser-assisted tunneling

Study laser-assisted tunneling in the presence of a magnet field gradient

- Initial state: atoms (^{87}Rb) in 3D lattice only populate even sites

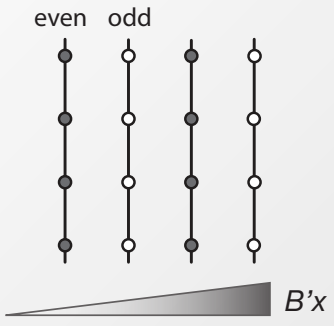

M. Aidelsburger *et al.*, PRL **111**, 185301 (2013)
similar work: H. Miyake *et al.*, PRL **111**, 185302 (2013)

Laser-assisted tunneling

Study laser-assisted tunneling in the presence of a magnet field gradient

• Initial state: atoms (^{87}Rb) in 3D lattice only populate even sites

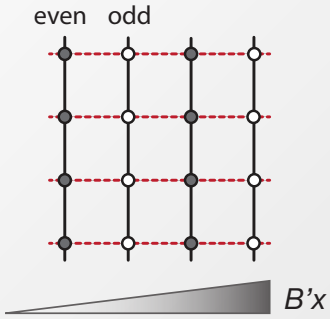

M. Aidelsburger *et al.*, PRL **111**, 185301 (2013)
similar work: H. Miyake *et al.*, PRL **111**, 185302 (2013)

Uniform flux

Laser-assisted tunneling

Study laser-assisted tunneling in the presence of a magnet field gradient

• Initial state: atoms (^{87}Rb) in 3D lattice only populate even sites

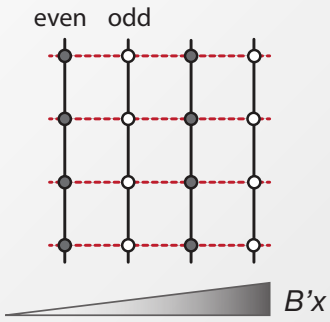

• Atom population in odd sites vs. modulation frequency

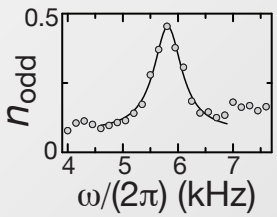

M. Aidelsburger *et al.*, PRL **111**, 185301 (2013)
similar work: H. Miyake *et al.*, PRL **111**, 185302 (2013)

Sunday 22 June 14

Laser-assisted tunneling

Study laser-assisted tunneling in the presence of a magnet field gradient

- Initial state: atoms (^{87}Rb) in 3D lattice only populate even sites

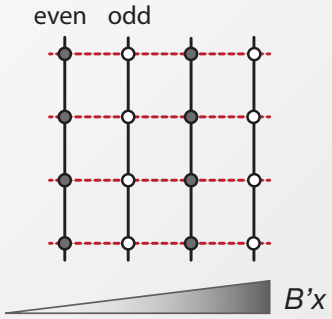

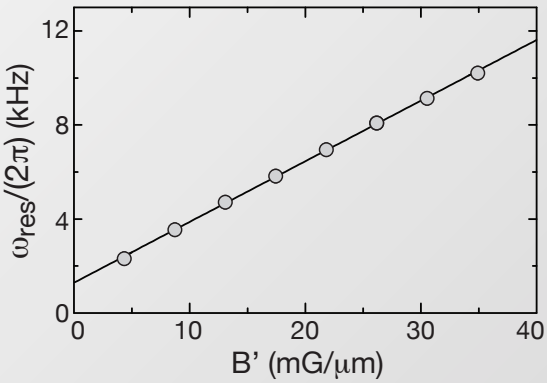

- Atom population in odd sites vs. modulation frequency

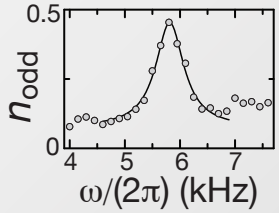

Large range of values accessible!

M. Aidelsburger *et al.*, PRL **111**, 185301 (2013)
similar work: H. Miyake *et al.*, PRL **111**, 185302 (2013)

Hamiltonian

Realization of the Hofstadter-Harper Hamiltonian

$$\hat{H} = -\sum_{m,n} \left(K \mathrm{e}^{i\phi_{m,n}} \hat{a}^{\dagger}_{m+1,n} \hat{a}_{m,n} + J \hat{a}^{\dagger}_{m,n+1} \hat{a}_{m,n} \right) + \mathrm{h.c.}$$

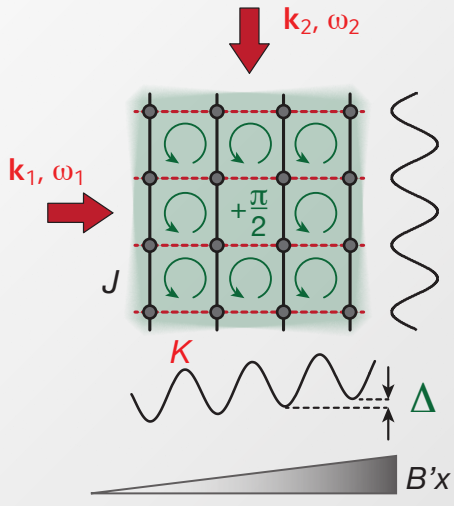

Scheme allows for the realization of an effective uniform flux of

$$\Phi = \pi/2$$

M. Aidelsburger *et al.*, PRL **111**, 185301 (2013)
similar work: H. Miyake *et al.*, PRL **111**, 185302 (2013)

Local observable

- **Classical:**

  Charged particle in magnetic field

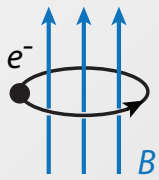

Local observable

- **Classical:**

  Charged particle in magnetic field

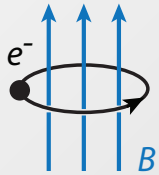

- **Quantum Analogue:**
  - Initial State:
  - Single Atom in the ground state of a tilted plaquette.

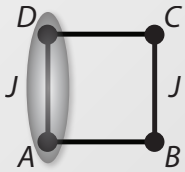

$$|\psi_0\rangle = \frac{|A\rangle + |D\rangle}{\sqrt{2}}$$

Local observable

- **Classical:**

  Charged particle in magnetic field

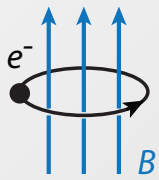

- **Quantum Analogue:**
  - Initial State:
  - Single Atom in the ground state of a tilted plaquette.

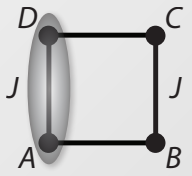

$$|\psi_0\rangle = \frac{|A\rangle + |D\rangle}{\sqrt{2}}$$

  - Switch on running-wave to induce tunneling

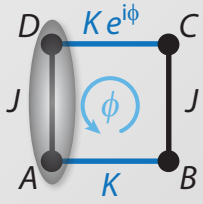

A Lattice of Plaquettes

Using two superlattices, we realize a lattice whose elementary cell is a 4-site plaquette.

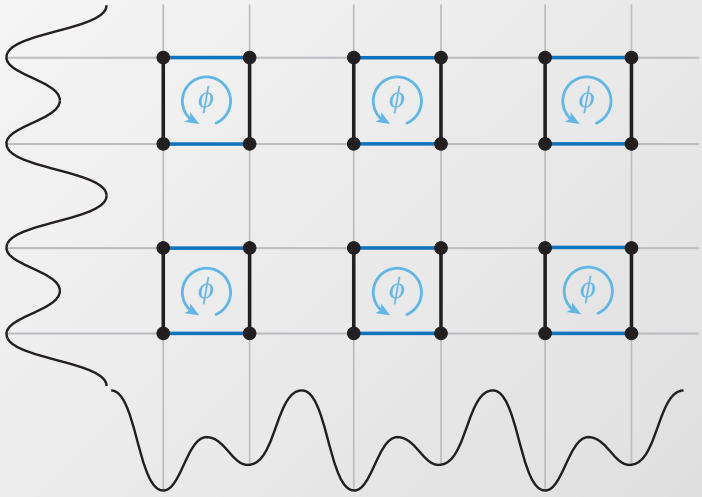

Mean atom position

- Site resolved detection along one direction

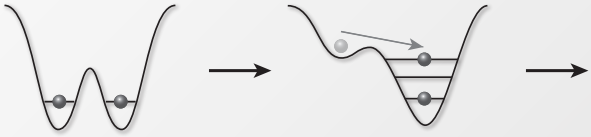

S. Fölling *et al.*, Nature (2007); J. Sebby-Strabley *et al.*, PRL (2007)

Uniform flux

Mean atom position

- Site resolved detection along one direction

band-
mapping

S. Fölling *et al.*, Nature (2007); J. Sebby-Strabley *et al.*, PRL (2007)

- Site resolved detection in plaquettes

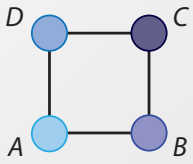

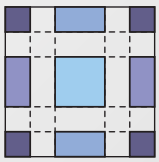

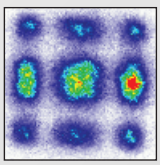

Sunday 22 June 14

Mean atom position

- Site resolved detection along one direction

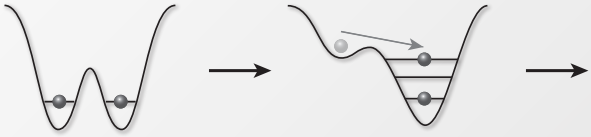

S. Fölling *et al.*, Nature (2007); J. Sebby-Strabley *et al.*, PRL (2007)

- Site resolved detection in plaquettes

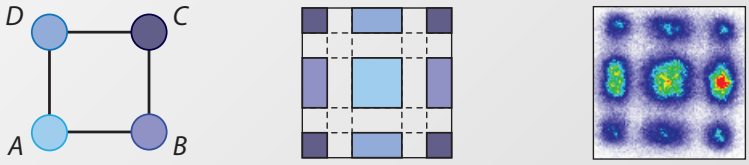

- Mean atom position along *x* and *y*

$$\frac{\langle X\rangle}{d_x} = \frac{-N_A + N_B + N_C - N_D}{2N} \quad \text{and} \quad \frac{\langle Y\rangle}{d_y} = \frac{-N_A - N_B + N_C + N_D}{2N}$$

Cyclotron orbit

Quantum analogue of cyclotron orbit

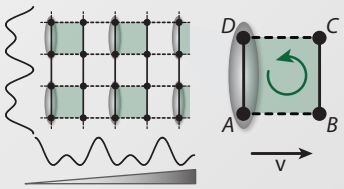

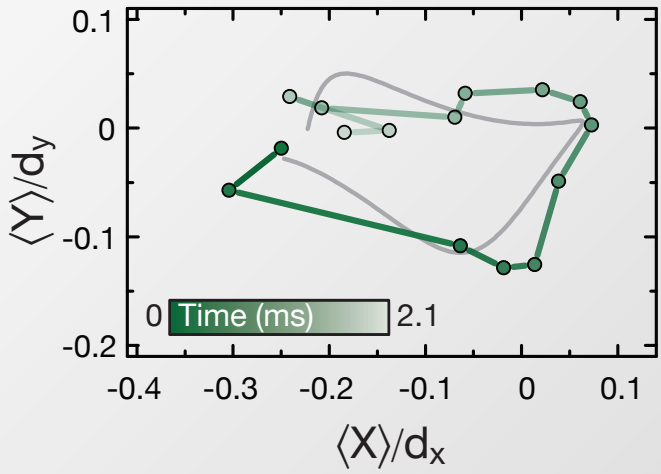

Parameters:

$$J/h = 0.5\,\text{kHz}$$
$$K/h = 0.3\,\text{kHz}$$
$$\Delta/h = 4.5\,\text{kHz}$$

Uniformity of the flux

Observation of the uniformity of the effective flux:

- Superlattice potential shifted by one lattice constant

Uniform flux

Uniformity of the flux

Observation of the uniformity of the effective flux:

- Superlattice potential shifted by one lattice constant

Sunday 22 June 14

Uniformity of the flux

Observation of the uniformity of the effective flux:

- Superlattice potential shifted by one lattice constant

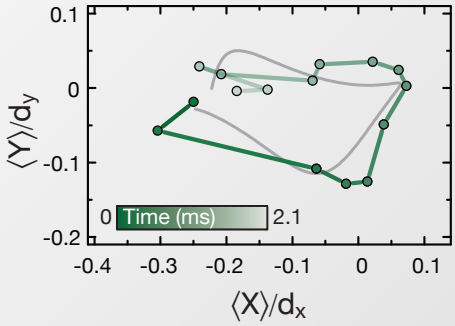

Uniform flux

Uniformity of the flux

Observation of the uniformity of the effective flux:

- Superlattice potential shifted by one lattice constant

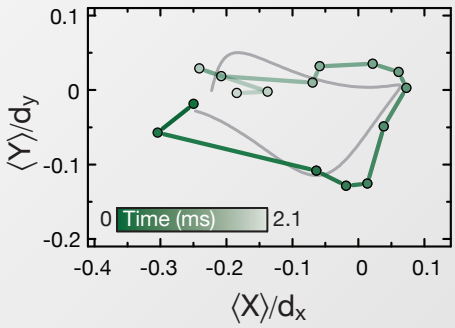

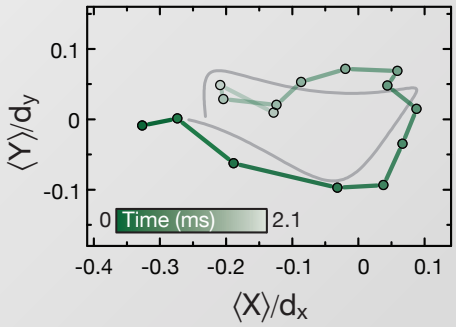

Uniformity of the flux

Observation of the uniformity of the effective flux:

• Superlattice potential shifted by one lattice constant

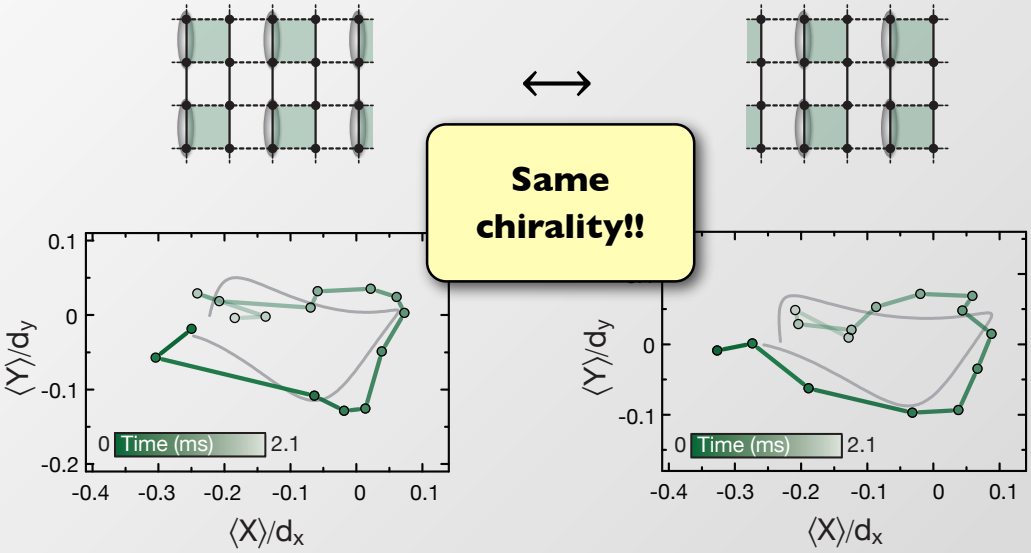

Quantum Spin Hall Hamiltonian

Value of the flux depends on the internal state of the atom

- $|\uparrow\rangle = |F = 1, m_F = -1\rangle$

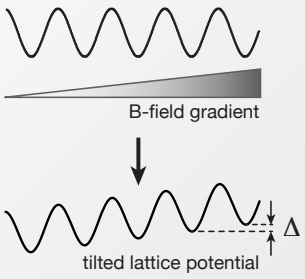

Quantum Spin Hall Hamiltonian

Value of the flux depends on the internal state of the atom

- $|\uparrow\rangle = |F = 1, m_F = -1\rangle$
- $|\downarrow\rangle = |F = 2, m_F = -1\rangle$

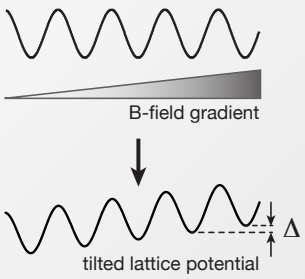

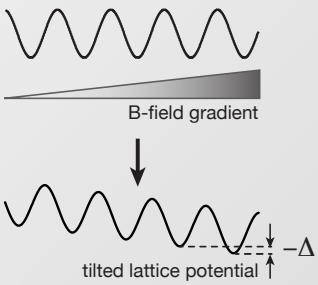

Uniform flux

Quantum Spin Hall Hamiltonian

Value of the flux depends on the internal state of the atom

- $|\uparrow\rangle = |F = 1, m_F = -1\rangle$
- $|\downarrow\rangle = |F = 2, m_F = -1\rangle$

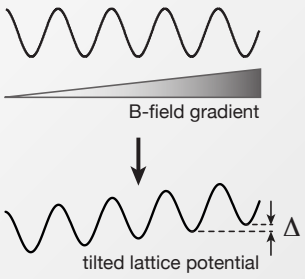

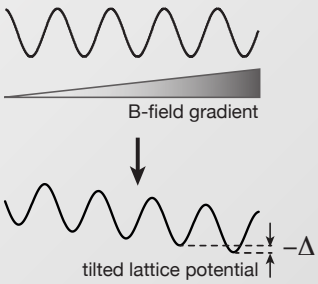

Spin-dependent optical potential: $\Delta \Longleftrightarrow -\Delta$

Sunday 22 June 14

Quantum Spin Hall Hamiltonian

Value of the flux depends on the internal state of the atom

- $|\uparrow\rangle = |F = 1, m_F = -1\rangle$
- $|\downarrow\rangle = |F = 2, m_F = -1\rangle$

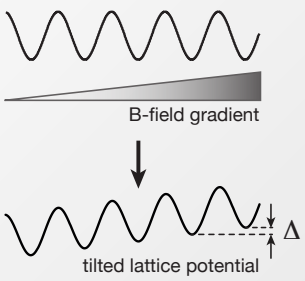

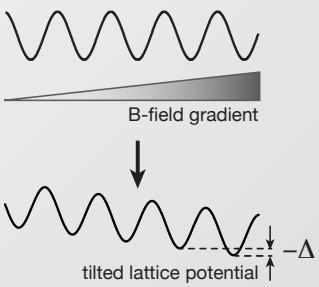

Spin-dependent optical potential: $\Delta \Longleftrightarrow -\Delta$

Spin-dependent complex tunneling amplitudes: $Ke^{i\phi_{mn}} \Longleftrightarrow Ke^{-i\phi_{mn}}$

Uniform flux

Quantum Spin Hall Hamiltonian

Value of the flux depends on the internal state of the atom

- $|\uparrow\rangle = |F = 1, m_F = -1\rangle$
- $|\downarrow\rangle = |F = 2, m_F = -1\rangle$

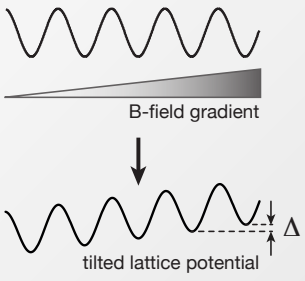

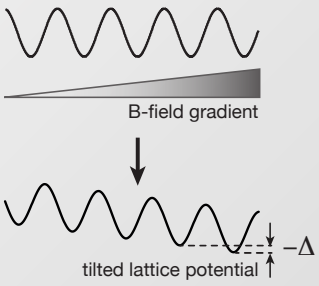

Spin-dependent optical potential: $\Delta \Longleftrightarrow -\Delta$

Spin-dependent complex tunneling amplitudes: $Ke^{i\phi_{mn}} \Longleftrightarrow Ke^{-i\phi_{mn}}$

Spin-dependent effective magnetic field: $\Phi = \pi/2 \Longleftrightarrow \Phi = -\pi/2$

Uniform flux

Quantum Spin Hall Hamiltonian

Time-reversal-symmetric quantum spin Hall Hamiltonian:

$$\hat{H}_{\uparrow,\downarrow} = -\sum_{m,n}\left(K\mathrm{e}^{\pm i\phi_{m,n}}\hat{a}^{\dagger}_{m+1,n}\hat{a}_{m,n} + J\hat{a}^{\dagger}_{m,n+1}\hat{a}_{m,n}\right) + \mathrm{h.c.}$$

Bernevig and Zhang, PRL **96**, 106802 (2006); N. Goldman *et al.*, PRL (2010)

Uniform flux

Quantum Spin Hall Hamiltonian

Time-reversal-symmetric quantum spin Hall Hamiltonian:

$$\hat{H}_{\uparrow,\downarrow} = -\sum_{m,n}\left(K\mathrm{e}^{\pm i\phi_{m,n}}\hat{a}^{\dagger}_{m+1,n}\hat{a}_{m,n} + J\hat{a}^{\dagger}_{m,n+1}\hat{a}_{m,n}\right) + \mathrm{h.c.}$$

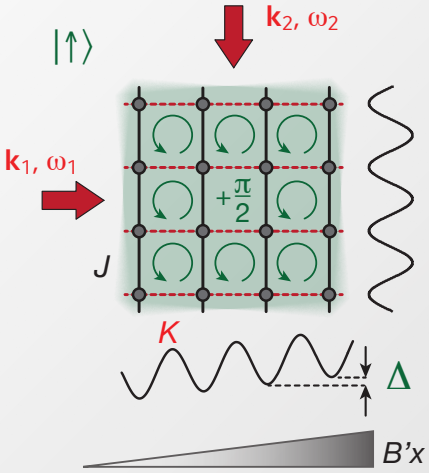

$$\Phi_{\uparrow} = \pi/2$$

Bernevig and Zhang, PRL **96**, 106802 (2006); N. Goldman *et al.*, PRL (2010)

Quantum Spin Hall Hamiltonian

Time-reversal-symmetric quantum spin Hall Hamiltonian:

$$\hat{H}_{\uparrow,\downarrow} = -\sum_{m,n}\left(K\mathrm{e}^{\pm i\phi_{m,n}}\hat{a}^{\dagger}_{m+1,n}\hat{a}_{m,n} + J\hat{a}^{\dagger}_{m,n+1}\hat{a}_{m,n}\right) + \mathrm{h.c.}$$

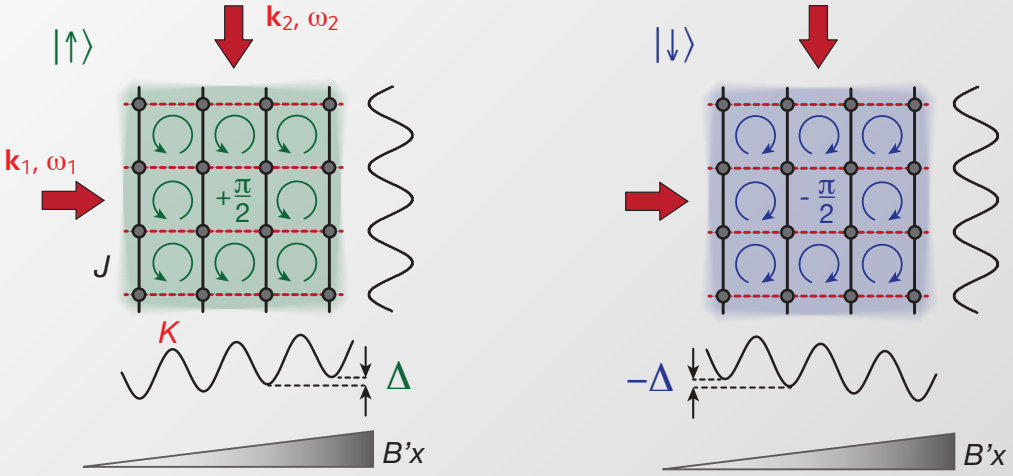

$\Phi_{\uparrow} = \pi/2$ $\Phi_{\downarrow} = -\pi/2$

Bernevig and Zhang, PRL **96**, 106802 (2006); N. Goldman *et al.*, PRL (2010)

Spin-dependent cyclotron orbit

- Spin up:

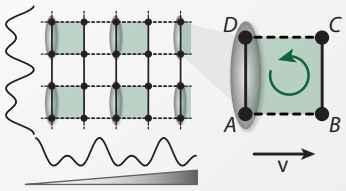

$$|\Psi_{\uparrow}\rangle = (|A\rangle + |D\rangle)/\sqrt{2}$$

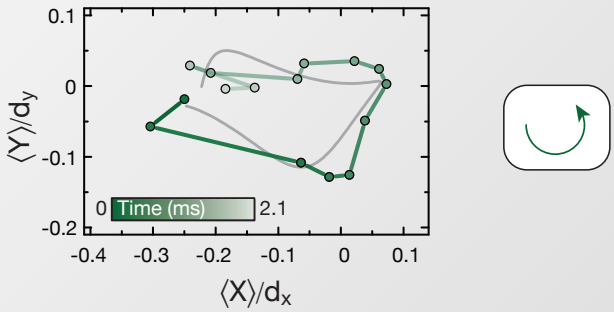

Spin-dependent cyclotron orbit

- Spin up:

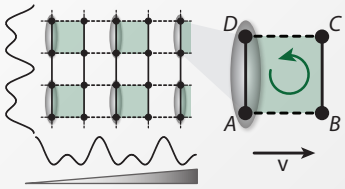

$$|\Psi_\uparrow\rangle = (|A\rangle + |D\rangle)/\sqrt{2}$$

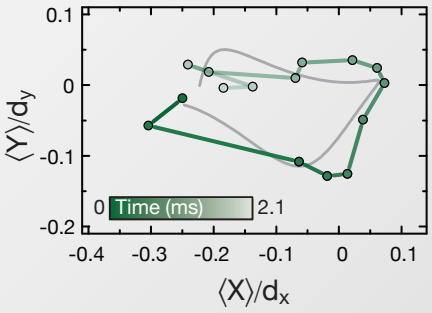

- Spin down:

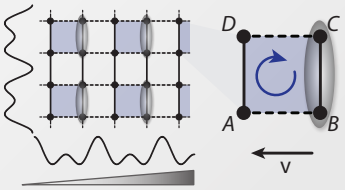

$$|\Psi_\downarrow\rangle = (|B\rangle + |C\rangle)/\sqrt{2}$$

Uniform flux

Spin-dependent cyclotron orbit

- Spin up:

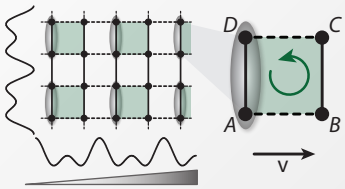

$$|\Psi_\uparrow\rangle = (|A\rangle + |D\rangle)/\sqrt{2}$$

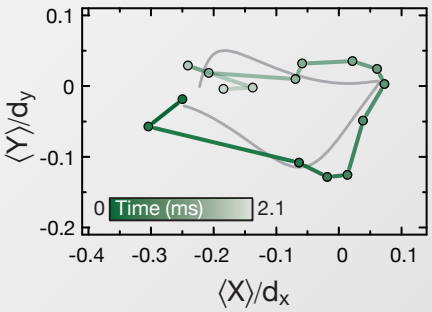

- Spin down:

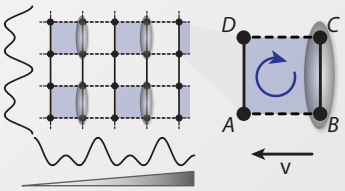

$$|\Psi_\downarrow\rangle = (|B\rangle + |C\rangle)/\sqrt{2}$$

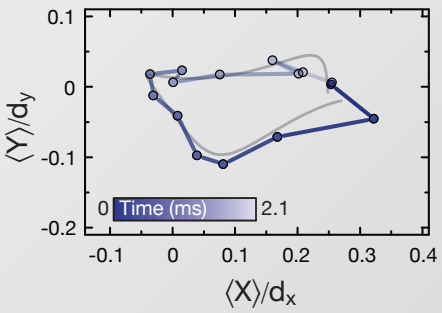

Sunday 22 June 14

Uniform flux

Spin-dependent cyclotron orbit

- Spin up:

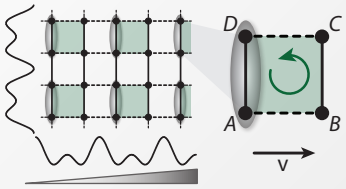

$$|\Psi_\uparrow\rangle = (|A\rangle + |D\rangle)/\sqrt{2}$$

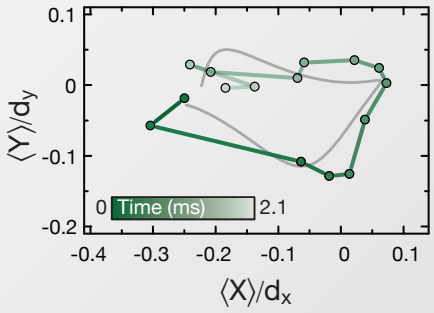

Opposite chirality!

- Spin down:

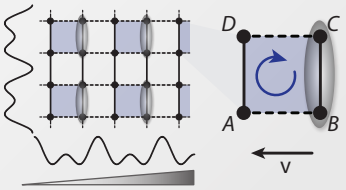

$$|\Psi_\downarrow\rangle = (|B\rangle + |C\rangle)/\sqrt{2}$$

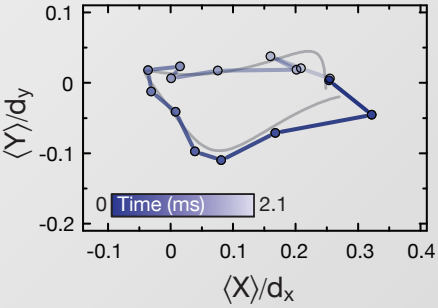

Sunday 22 June 14

Sunday 22 June 14

Flux ladder: experimental realization

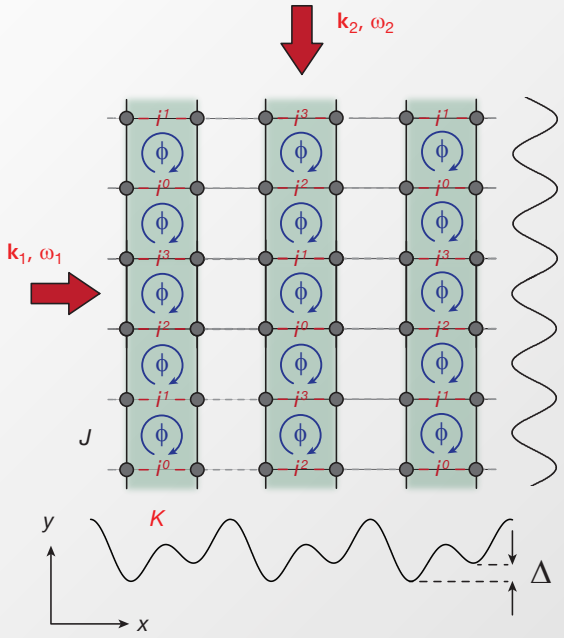

- resonant laser-assisted tunneling:

$$\omega_1 - \omega_2 = \Delta/\hbar$$

- Spatial dependent phase factors

$$\phi_n = n \cdot \pi/2$$

- Uniform flux

$$\Phi = \pi/2$$

Experiment: M. Atala et al., arXiv:1402.0819 (2014)
Theory: D. Hügel, B. Paredes, PRA 89, 023619 (2014)
E. Orignac & T. Giamarchi PRB 64, 144515 (2001)
A. Tokuno & A. Georges arXiv:1403.0413
R. Wei & E. Mueller arXiv:1405.0230

Flux Ladder

Flux ladder: experimental realization

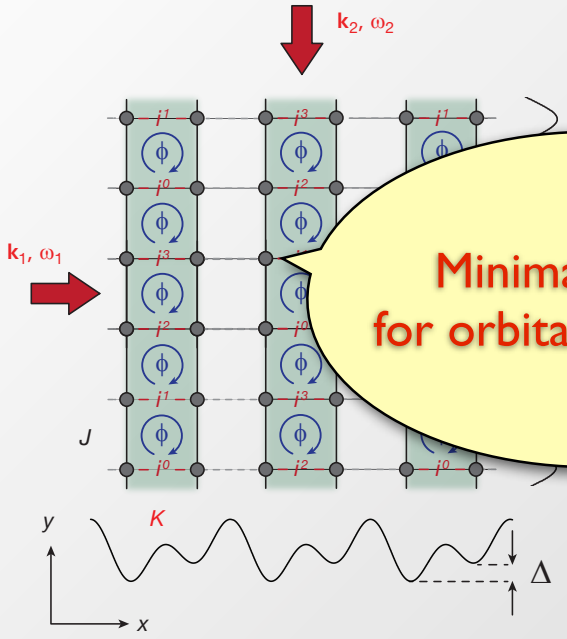

- resonant laser-assisted tunneling:

$$\omega_1 - \omega_2 = \Delta/\hbar$$

dent phase factors

$\cdot \pi/2$

ux

$$\Phi = \pi/2$$

Experiment: M. Atala et al., arXiv:1402.0819 (2014)
Theory: D. Hügel, B. Paredes, PRA 89, 023619 (2014)
E. Orignac & T. Giamarchi PRB 64, 144515 (2001)
A. Tokuno & A. Georges arXiv:1403.0413
R. Wei & E. Mueller arXiv:1405.0230

Flux Ladder Hamiltonian

Hamiltonian of the system written in a simpler theory gauge

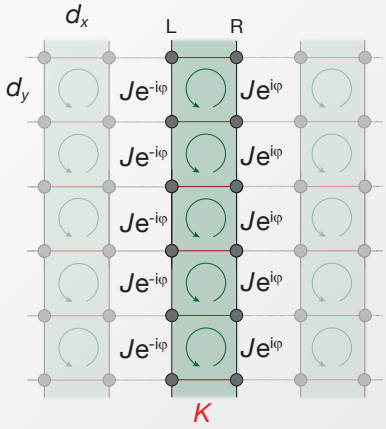

$$H = -J\sum_{\ell}\left(e^{-i\ell\varphi}\hat{a}^{\dagger}_{\ell+1;L}\hat{a}_{\ell;L} + e^{i\ell\varphi}\hat{a}^{\dagger}_{\ell+1;R}\hat{a}_{\ell;R}\right)$$
$$-K\sum_{\ell}\left(\hat{a}^{\dagger}_{\ell;L}\hat{a}_{\ell;R}\right) + \text{h.c.}$$

Flux: $\phi = 2\varphi$

Flux Ladder Hamiltonian

Hamiltonian of the system written in a simpler theory gauge

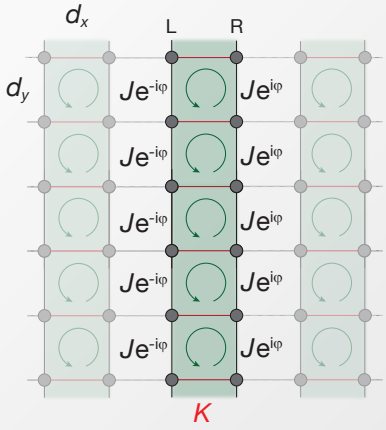

$$H = -J\sum_{\ell}\left(e^{-i\ell\varphi}\hat{a}^{\dagger}_{\ell+1;L}\hat{a}_{\ell;L} + e^{i\ell\varphi}\hat{a}^{\dagger}_{\ell+1;R}\hat{a}_{\ell;R}\right)$$
$$-K\sum_{\ell}\left(\hat{a}^{\dagger}_{\ell;L}\hat{a}_{\ell;R}\right) + \text{h.c.}$$

Flux: $\phi = 2\varphi$

Define: $\hat{a}_{q;\mu} = \sum_{\ell} e^{iq\ell}\hat{a}_{\ell;\mu},$

and solve for the ansatz $|\psi_q\rangle = (\alpha_q\hat{a}^{\dagger}_{q;L} + \beta_q\hat{a}^{\dagger}_{q;R})\,|0\rangle$

Ladder Band Structure

$$\epsilon_q = 2J\cos(q)\cos(\varphi) \pm \sqrt{K^2 - 4J^2\sin^2(\varphi)\sin^2(q)}$$

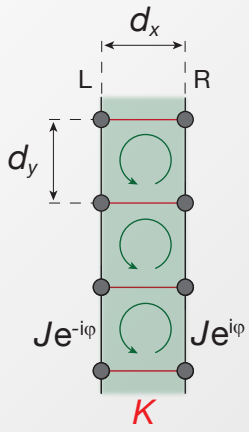

Ladder Band Structure

Two energy bands

$$\epsilon_q = 2J\cos(q)\cos(\varphi) \pm \sqrt{K^2 - 4J^2\sin^2(\varphi)\sin^2(q)}$$

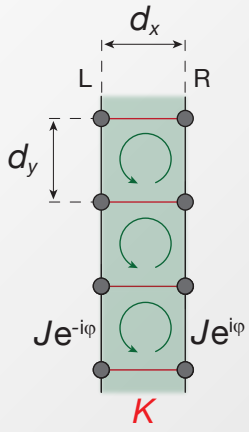

Ladder Band Structure

Two energy bands

$$\epsilon_q = 2J\cos(q)\cos(\varphi) \pm \sqrt{K^2 - 4J^2\sin^2(\varphi)\sin^2(q)}$$

$\phi = 2\varphi = \pi/2$

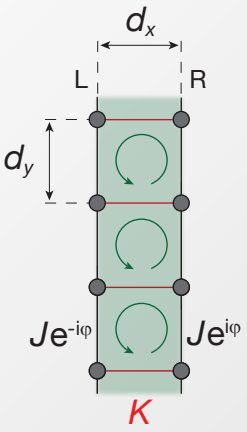

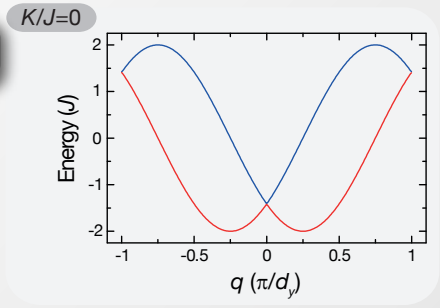

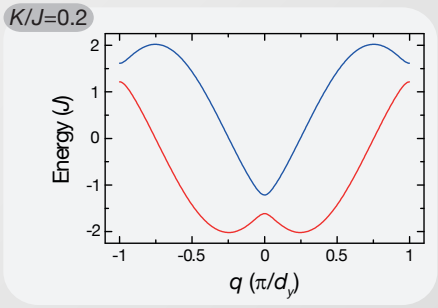

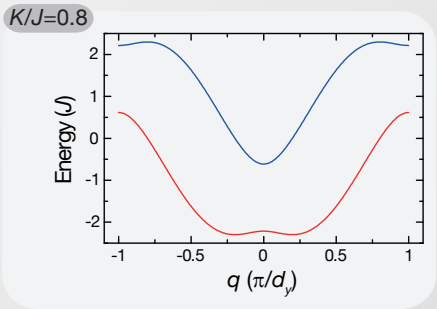

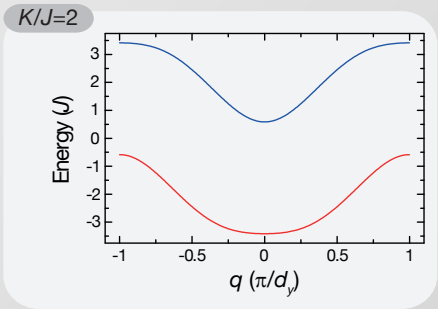

Flux Ladder

Ladder Band Structure

Two energy bands

$$\epsilon_q = 2J\cos(q)\cos(\varphi) \pm \sqrt{K^2 - 4J^2\sin^2(\varphi)\sin^2(q)}$$

$\phi = 2\varphi = \pi/2$

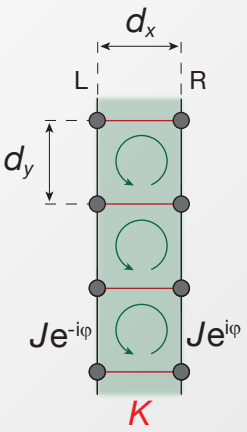

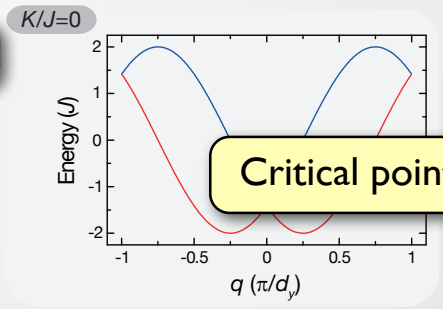

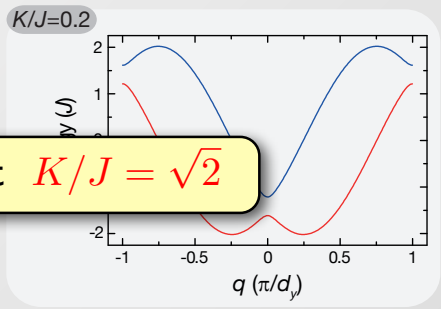

Critical point at $K/J = \sqrt{2}$

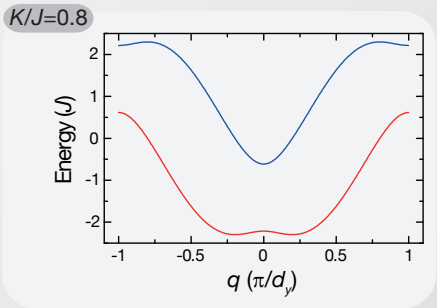

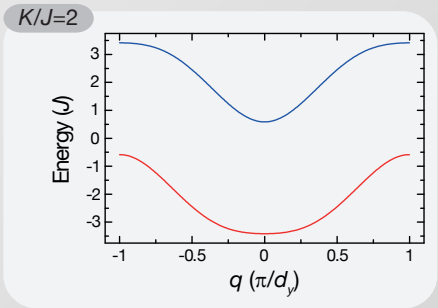

Probability Currents in Ladder

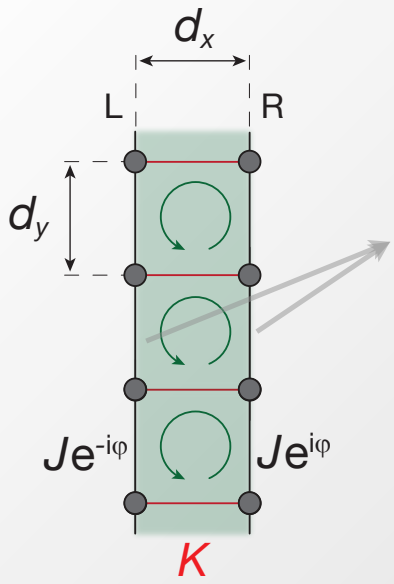

Current along the legs:

$$\hat{\mathbf{j}}^{y}_{\ell;\mu} = -\frac{i}{\hbar}\left(\hat{a}^{\dagger}_{\ell+1;\mu}\hat{a}_{\ell;\mu}H_{\ell\to\ell+1;\mu} - \text{h.c}\right)$$

$$\mu = (\text{L=left,R=right})$$

In the experiment ***total current*** is measured

$$\mathbf{j}_{\mathrm{L}} = N_{leg}^{-1}\sum_{l}\mathbf{j}^{y}_{l;L}$$

Chiral current: $\mathbf{j}_{\mathrm{C}} = \mathbf{j}_{\mathrm{L}} - \mathbf{j}_{\mathrm{R}}$

Phase Diagram

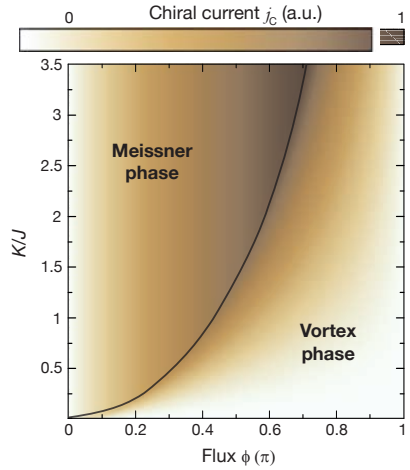

see E. Orignac & T. Giamarchi PRB 64, 144515 (2001)

Phase Diagram

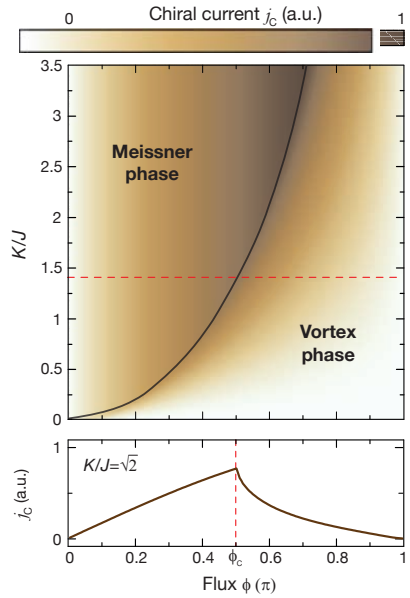

see E. Orignac & T. Giamarchi PRB 64, 144515 (2001)

Phase Diagram

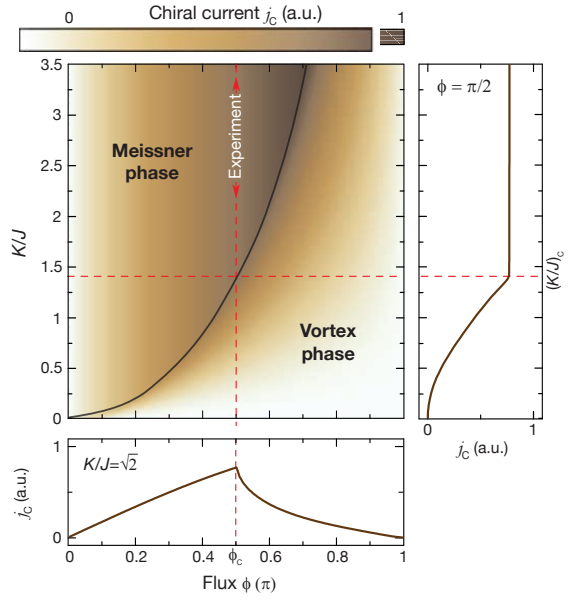

see E. Orignac & T. Giamarchi PRB 64, 144515 (2001)

Phase Diagram

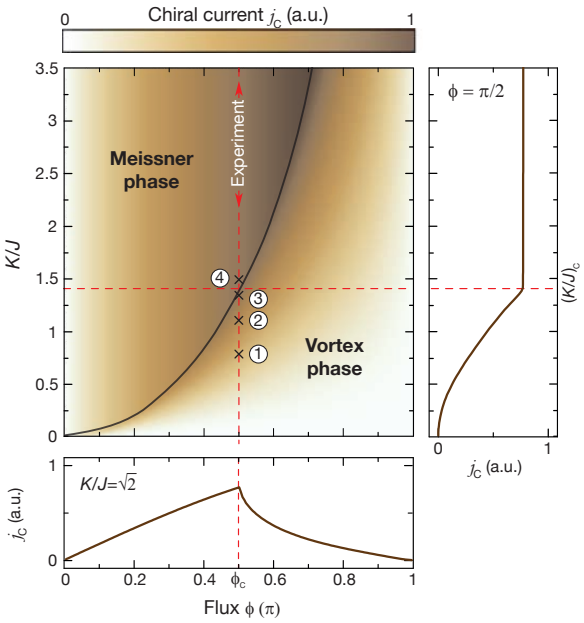

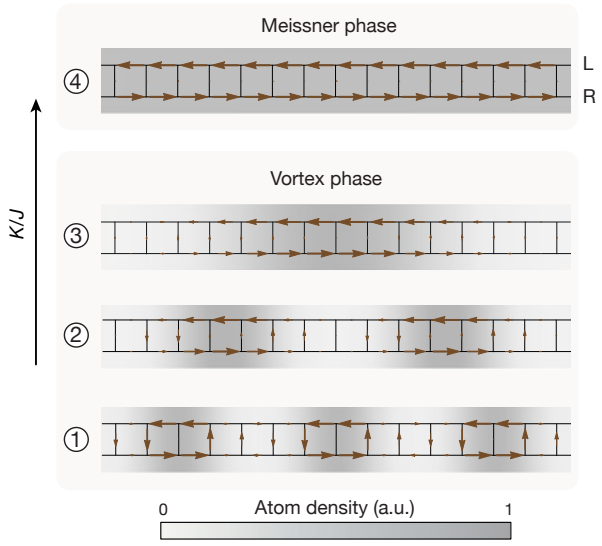

see E. Orignac & T. Giamarchi PRB 64, 144515 (2001)

Spin-orbit coupling - short digression

- The flux ladder Hamiltonian can be mapped into a spin-orbit coupled system
- Left right legs are mapped into pseudo-spins:

$$\hat{a}_{\ell;R} \rightarrow \hat{a}_{\ell;\downarrow} \qquad \hat{a}_{\ell;L} \rightarrow \hat{a}_{\ell;\uparrow}$$

Spin-Momentum locking: D. Hügel, B. Paredes, PRA 89, 023619 (2014)

Continuum: I. B. Spielman Nature 471, 83 (2011)

Spin-orbit coupling - short digression

- The flux ladder Hamiltonian can be mapped into a spin-orbit coupled system
- Left right legs are mapped into pseudo-spins:

$$\hat{a}_{\ell;R} \rightarrow \hat{a}_{\ell;\downarrow} \qquad \hat{a}_{\ell;L} \rightarrow \hat{a}_{\ell;\uparrow}$$

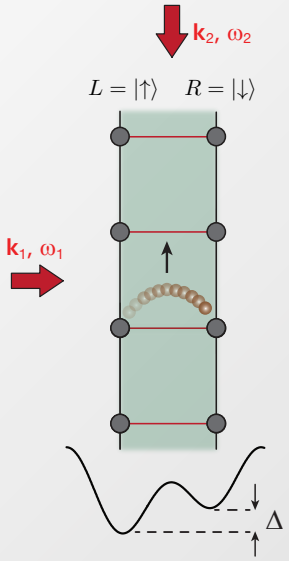

Spin-Momentum locking: D. Hügel, B. Paredes, PRA 89, 023619 (2014)

Continuum: I. B. Spielman Nature 471, 83 (2011)

Flux ladder

Spin-orbit coupling - short digression

- The flux ladder Hamiltonian can be mapped into a spin-orbit coupled system
- Left right legs are mapped into pseudo-spins:

$$\hat{a}_{\ell;R} \rightarrow \hat{a}_{\ell;\downarrow} \qquad \hat{a}_{\ell;L} \rightarrow \hat{a}_{\ell;\uparrow}$$

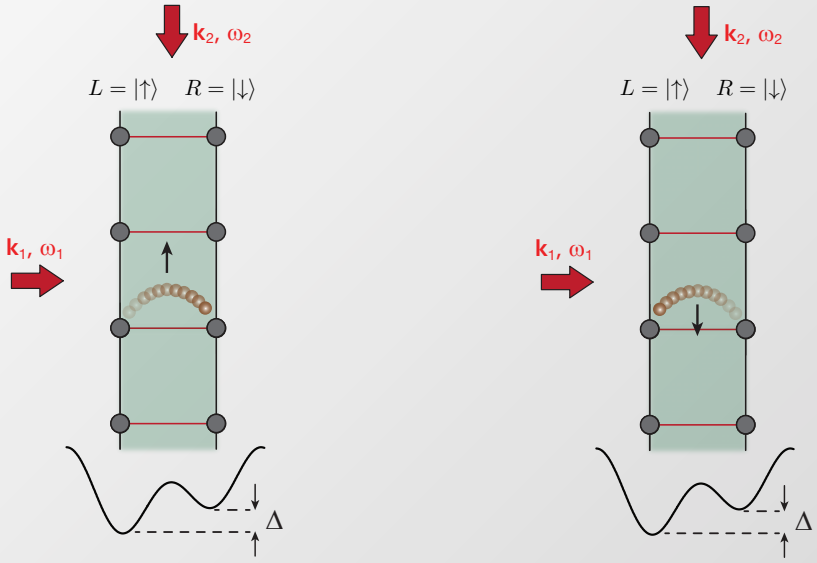

Spin-Momentum locking: D. Hügel, B. Paredes, PRA 89, 023619 (2014)

Continuum: I. B. Spielman Nature 471, 83 (2011)

Sunday 22 June 14

Spin-orbit coupling - short digression

- The flux ladder Hamiltonian can be mapped into a spin-orbit coupled system
- Left right legs are mapped into pseudo-spins:

$$\hat{a}_{\ell;R} \rightarrow \hat{a}_{\ell;\downarrow} \qquad \hat{a}_{\ell;L} \rightarrow \hat{a}_{\ell;\uparrow}$$

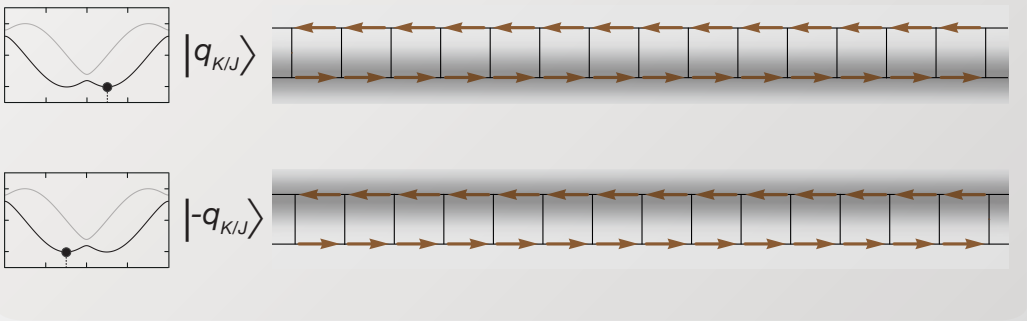

Spin-Momentum locking: D. Hügel, B. Paredes, PRA 89, 023619 (2014)

Continuum: I. B. Spielman Nature 471, 83 (2011)

Current Measurements: Sequence

How to measure currents in our setup?

→ *project the state into isolated double wells*

S. Trotzky *et al.* Nature Physics 8, 325 (2012)
S. Kessler & F. Marquardt, arXiv:1309.3890 (2012)

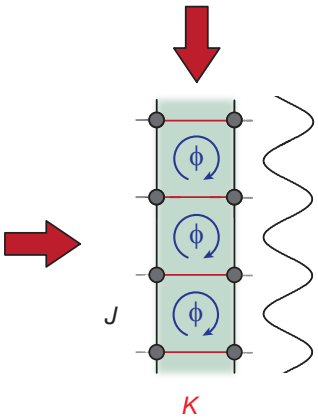

Groundstate

Josephson oscillations in double wells

Current Measurements: Sequence

How to measure currents in our setup?

→ *project the state into isolated double wells*

S. Trotzky *et al.* Nature Physics 8, 325 (2012)
S. Kessler & F. Marquardt, arXiv:1309.3890 (2012)

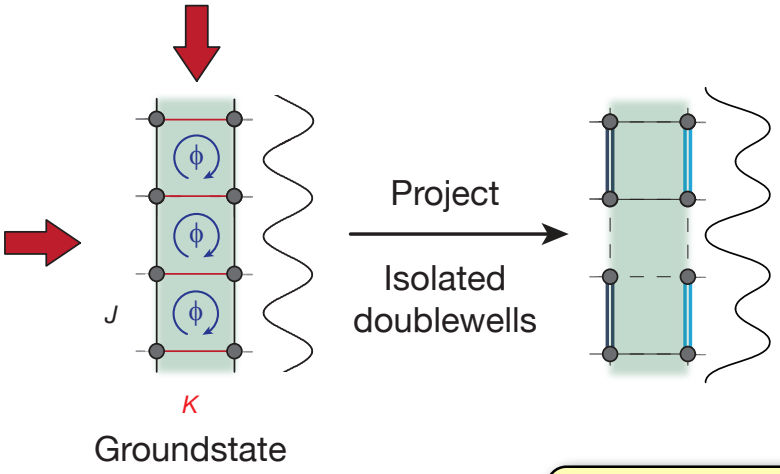

Josephson oscillations in double wells

Flux Ladder

Current Measurements: Sequence

How to measure currents in our setup?

→ *project the state into isolated double wells*

S. Trotzky *et al.* Nature Physics 8, 325 (2012)
S. Kessler & F. Marquardt, arXiv:1309.3890 (2012)

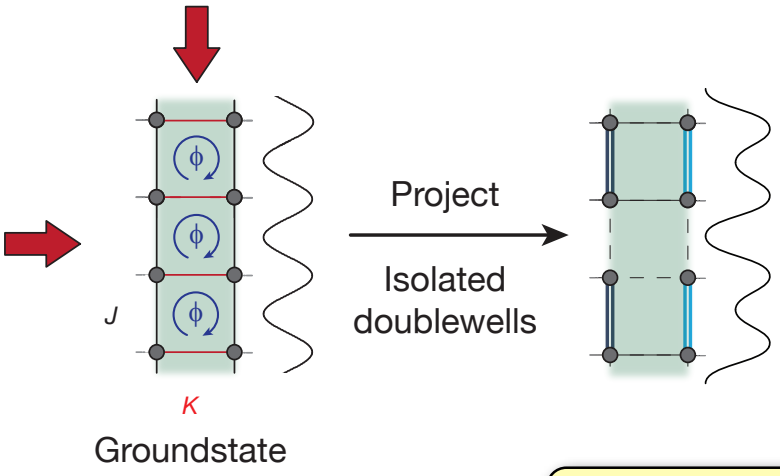

- Hold in double wells for a time *t*

Josephson oscillations in double wells

Current Measurements: Sequence

How to measure currents in our setup?

→ *project the state into isolated double wells*

S. Trotzky *et al.* Nature Physics 8, 325 (2012)
S. Kessler & F. Marquardt, arXiv:1309.3890 (2012)

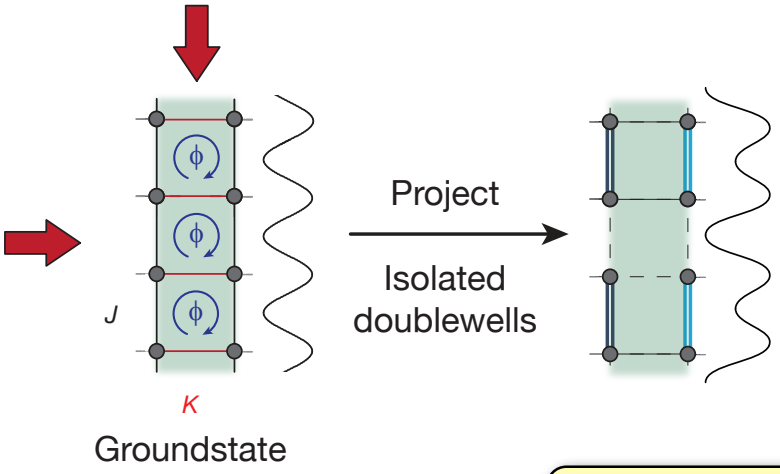

- Hold in double wells for a time *t*
- Measure *even-odd population* in double well

Josephson oscillations in double wells

Double well oscillations - currents

In the experiment we measure the average of all the oscillations on either side of the ladder:

$$n_{\mathrm{even};\mu}(t) = \frac{1}{2}[1 + (n_{\mathrm{even};\mu}(0) - n_{\mathrm{odd};\mu}(0))\cos(2\omega t) - \frac{j_\mu}{J/\hbar}\sin(2\omega t)]$$

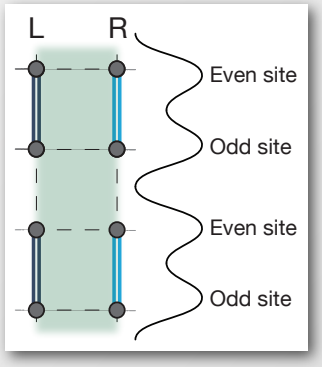

Oscillations in double wells

• Prepare ground state of the flux ladder with K/J=2 and project into isolated double wells

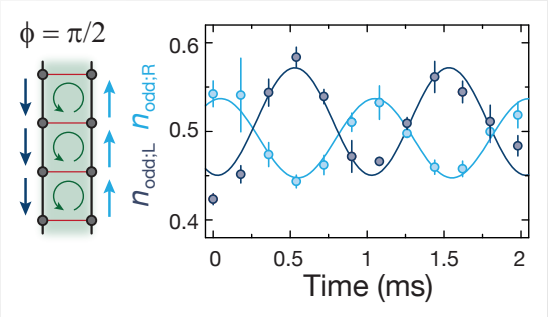

Oscillations in double wells

• Prepare ground state of the flux ladder with K/J=2 and project into isolated double wells

Reversed flux

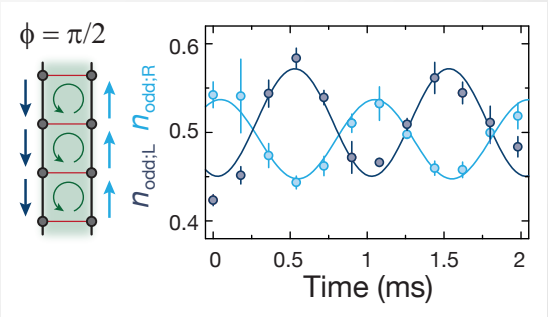

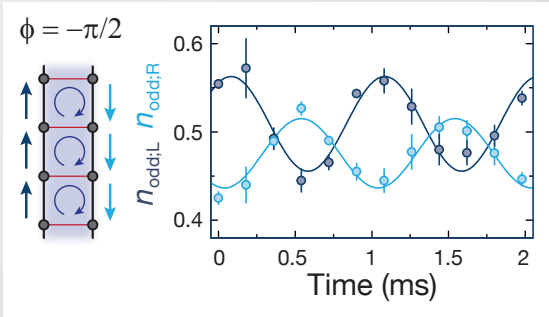

When inverting the flux the current gets reversed

Zero flux ladders

- Prepare ground state of the ladder with zero flux
- project into isolated double wells

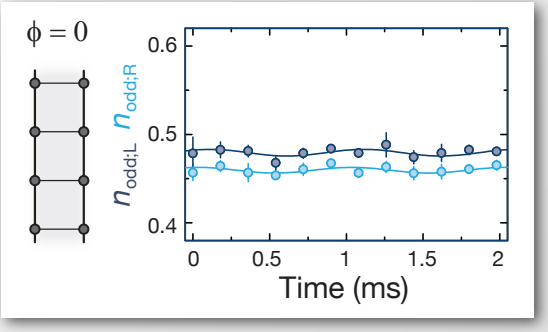

Extracting the Chiral current

The chiral current can be reliably calculated by

$$n_{\mathrm{even};\mu}(t) = \frac{1}{2}[1 + (n_{\mathrm{even};\mu}(0) - n_{\mathrm{odd};\mu}(0))\cos(2\omega t) - \frac{j_\mu}{J/\hbar}\sin(2\omega t)]$$

$$n_{\mathrm{even;L}}(t) - n_{\mathrm{even;R}}(t) = \frac{\mathbf{j}_C}{J/\hbar}\sin(2\omega t)$$

Extracting the Chiral current

The chiral current can be reliably calculated by

$$n_{\mathrm{even;L}}(t) - n_{\mathrm{even;R}}(t) = \frac{\mathbf{j}_C}{J/\hbar}\sin(2\omega t)$$

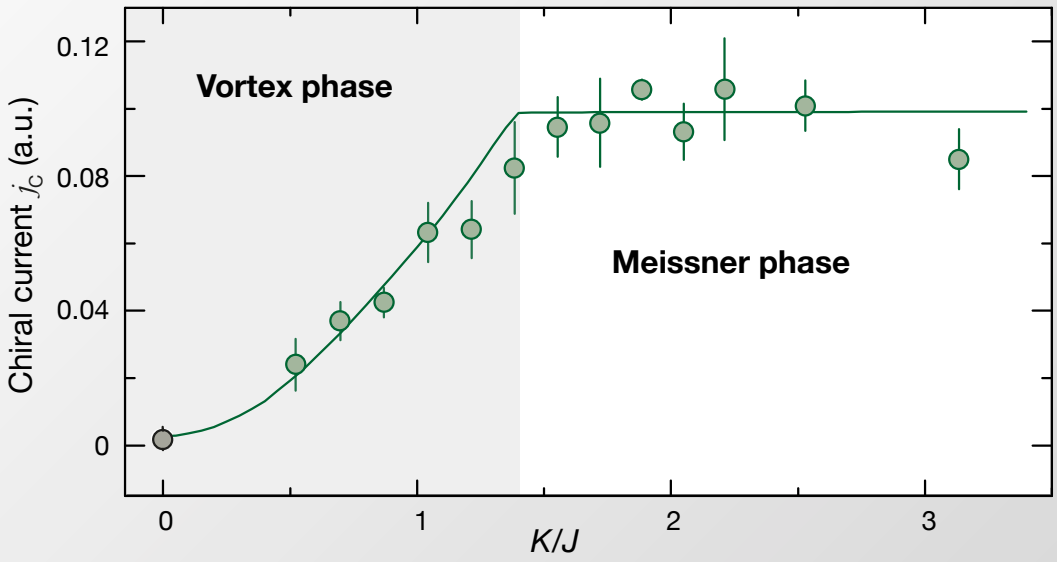

Experimental Results - Momentum Distribution

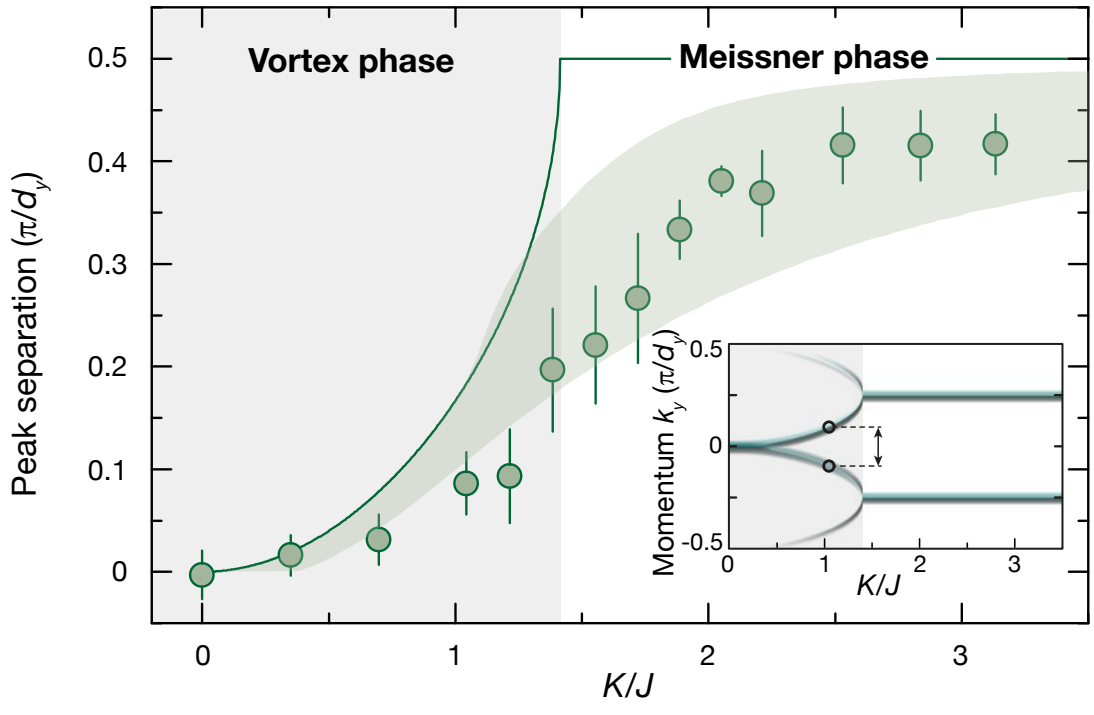

Summary and Outlook

- ***New detection method*** for probability currents
- Measurement of ***Chiral Edge States*** in Ladders
- Identification of ***Meissner-like effect in bosonic ladder***

Outlook:

- Entering the strongly correlated regime
- Chiral Mott Insulators
- Spin Meissner effect
- Connection of chiral ladder states to Hoftstadter model edge states
- Spin-Orbit Coupling in 1D

E. Orignac & T. Giamarchi PRB 64, 144515 (2001)
Dhar, A *et al.*, PRA 85, 041602 (2012)
Petrescu, A. & Le Hur, K. PRL 111, 150601 (2013)
A Tokuno & A Georges, arXiv:1403.0413

Probing Band Topology

Measuring the Zak-Berry's Phase of Topological Bands

M. Atala et al., Nature Physics (2013)

www.quantum-munich.de

Berry Phase in Quantum Mechanics

$$\Psi(R) \rightarrow e^{i(\varphi_{\mathrm{Berry}}+\varphi_{\mathrm{dyn}})}\ \Psi(R)$$

Adiabatic evolution through closed loop

$$\varphi_{\mathrm{Berry}} = \oint_{\mathcal{C}} A_n(R) dR = i \oint_{\mathcal{C}} \langle n(R)|\nabla_R|n(R)\rangle\, dR$$

$$\varphi_{\mathrm{Berry}} = \oint_{\mathcal{A}} \Omega_n(R)\, dA$$

Berry Phase

M.V. Berry, Proc. R. Soc. A (1984)

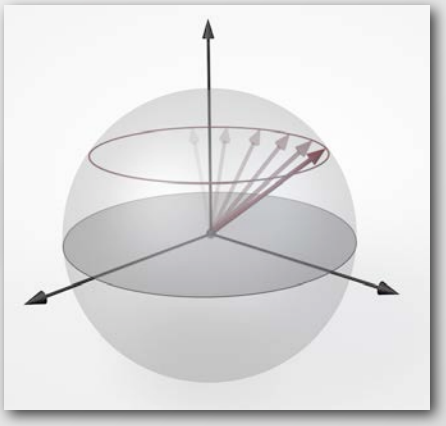

Example: Spin-1/2 particle in magnetic field

Berry connection

$$A_n(R) = i\langle n(R)|\nabla_R|n(R)\rangle$$

Berry curvature

$$\Omega_{n,\mu\nu}(R) = \frac{\partial}{\partial R^\mu} A_{n,\nu} - \frac{\partial}{\partial R^\nu} A_{n,\mu}$$

Berry Phase for Periodic Potentials

$$\Psi_k(\mathbf{r}) = e^{i\mathbf{kr}} u_k(\mathbf{r})$$ Bloch wave in periodic potential

Adiabatic motion in momentum space generates Berry phase!

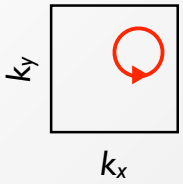

Mention Problem with going on a line is generally NOT A LOOP IN PARAMETER SPACE!

Berry Phase

Berry Phase for Periodic Potentials

$$\Psi_k(\mathbf{r}) = e^{i\mathbf{kr}} u_k(\mathbf{r})$$ Bloch wave in periodic potential

Adiabatic motion in momentum space generates Berry phase!

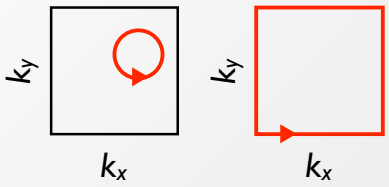

Mention Problem with going on a line is generally NOT A LOOP IN PARAMETER SPACE!

Sunday 22 June 14

Berry Phase for Periodic Potentials

$$\Psi_k(\mathbf{r}) = e^{i\mathbf{kr}} u_k(\mathbf{r})$$ Bloch wave in periodic potential

Adiabatic motion in momentum space generates Berry phase!

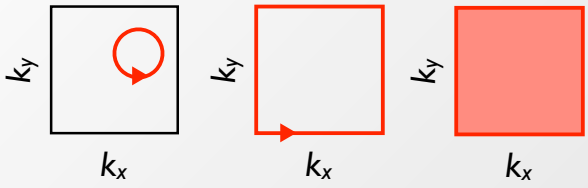

Mention Problem with going on a line is generally NOT A LOOP IN PARAMETER SPACE!

Berry Phase

Berry Phase for Periodic Potentials

$$\Psi_k(\mathbf{r}) = e^{i\mathbf{kr}} u_k(\mathbf{r})$$ Bloch wave in periodic potential

Adiabatic motion in momentum space generates Berry phase!

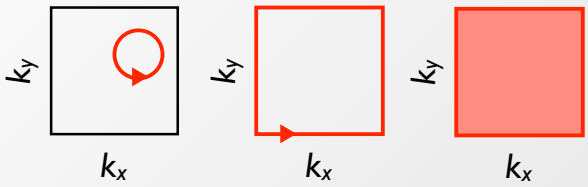

Berry phase is fundamental to characterize topology of energy bands

$$n_{\text{Chern}} = \frac{1}{2\pi}\oint_{BZ} A_k dk = \frac{1}{2\pi}\int_{BZ} \Omega_k \, d^2k \quad \Leftrightarrow \quad \sigma_{xy} = n_{\text{Chern}}\, e^2/h$$

Chern Number (Topological Invariant) **Quantized Hall Conductance**

Thouless, Kohmoto, den Nijs, and Nightingale (TKNN), PRL 1982
Kohmoto Ann. of Phys. 1985

Mention Problem with going on a line is generally NOT A LOOP IN PARAMETER SPACE!

Berry Phase for Periodic Potentials

$$\Psi_k(\mathbf{r}) = e^{i\mathbf{k}\mathbf{r}} u_k(\mathbf{r})$$ Bloch wave in periodic potential

Adiabatic motion in momentum space generates Berry phase!

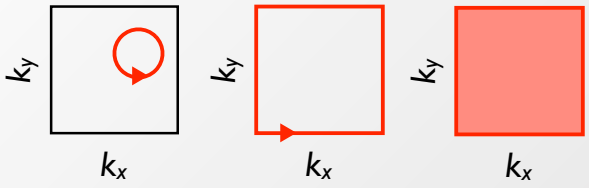

Berry phase is fundamental to characterize topology of energy bands

$$n_{\text{Chern}} = \frac{1}{2\pi}\oint_{BZ} A_k dk = \frac{1}{2\pi}\int_{BZ} \Omega_k \, d^2k \quad \Leftrightarrow \quad \sigma_{xy} = n_{\text{Chern}}\, e^2/h$$

Chern Number (Topological Invariant) **Quantized Hall Conductance**

Thouless, Kohmoto, den Nijs, and Nightingale (TKNN), PRL 1982
Kohmoto Ann. of Phys. 1985

What is the extension to 1D?

Mention Problem with going on a line is generally NOT A LOOP IN PARAMETER SPACE!

Zak Phase

2D Brillouin Zone

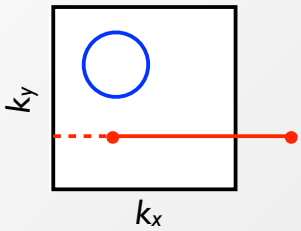

going straight means going around!

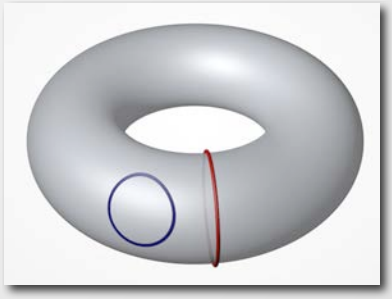

Band structure has torus topology!

Zak Phase

2D Brillouin Zone

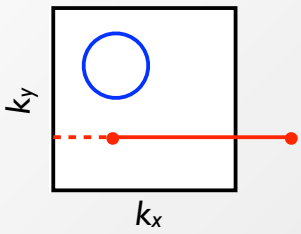

going straight means going around!

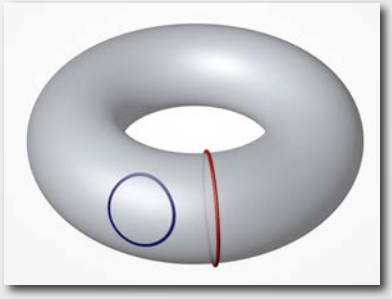

Band structure has torus topology!

$$\varphi_{Zak} = i \int_{k_0}^{k_0+G} \langle u_k | \partial_k | u_k \rangle \; dk$$

Zak Phase - the 1D Berry Phase

J. Zak, Phys. Rev. Lett. **62**, 2747 (1989)

Berry Phase

Zak Phase

2D Brillouin Zone

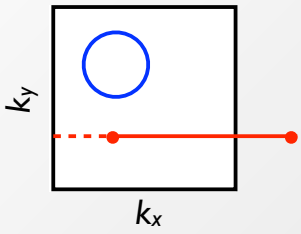

going straight means going around!

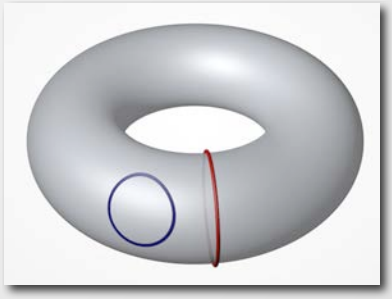

Band structure has torus topology!

$$\varphi_{Zak} = i \int_{k_0}^{k_0+G} \langle u_k | \partial_k | u_k \rangle \; dk$$

Zak Phase - the 1D Berry Phase

J. Zak, Phys. Rev. Lett. **62**, 2747 (1989)

Non-trivial Zak phase:

- Topological Band
- Edge States (for finite system)
- Domain walls with fractional quantum numbers

R. Jackiw and C. Rebbi, Phys. Rev. D 13, 3398 (1976)
J. Goldstone and F. Wilczek, Phys. Rev. Lett. 47, 986 (1981)

Su-Shrieffer-Heeger Model (SSH)

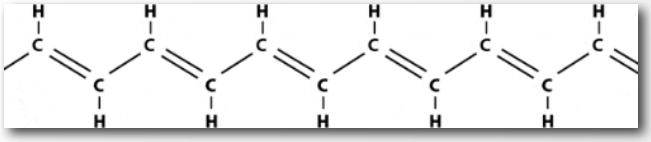

Polyacetylene

W. P. Su, J. R. Schrieffer & A. J. Heeger
Phys. Rev. Lett. 42, 1698 (1979).

$$H_{SSH} = -\sum_n \left\{ J\hat{a}_n^\dagger \hat{b}_n + J'\hat{a}_n^\dagger \hat{b}_{n-1} + \text{h.c.} \right\}$$

Su-Shrieffer-Heeger Model (SSH)

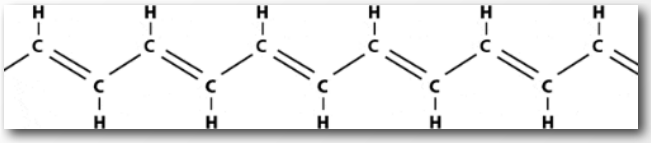

Polyacetylene

W. P. Su, J. R. Schrieffer & A. J. Heeger
Phys. Rev. Lett. 42, 1698 (1979).

$$H_{SSH} = -\sum_n \left\{ J\hat{a}_n^\dagger \hat{b}_n + J'\hat{a}_n^\dagger \hat{b}_{n-1} + \text{h.c.} \right\}$$

Two topologically distinct phases:

D1: $J > J'$

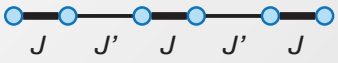

D2: $J' > J$

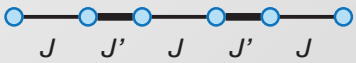

Su-Shrieffer-Heeger Model (SSH)

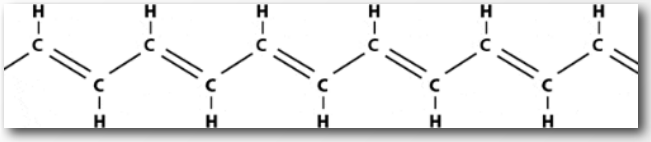

Polyacetylene

W. P. Su, J. R. Schrieffer & A. J. Heeger
Phys. Rev. Lett. 42, 1698 (1979).

$$H_{SSH} = -\sum_n \left\{ J\hat{a}_n^\dagger \hat{b}_n + J'\hat{a}_n^\dagger \hat{b}_{n-1} + \text{h.c.} \right\}$$

Two topologically distinct phases:

D1: $J > J'$

D2: $J' > J$

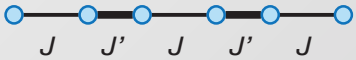

$$\delta\varphi_{Zak} = \varphi_{Zak}^{D1} - \varphi_{Zak}^{D2} = \pi$$

Topological properties:
domain wall features fractionalized excitations

Zak phase difference $\delta\varphi_{Zak}$ is gauge-invariant

SSH Energy Bands - Eigenstates

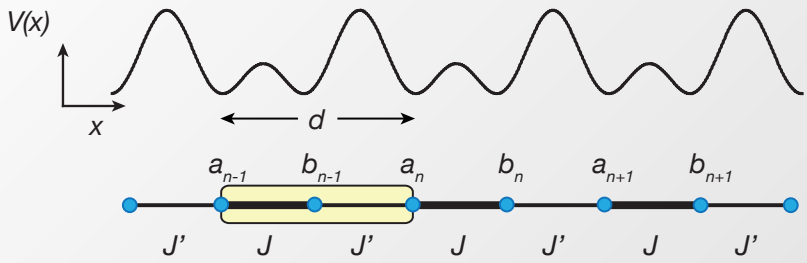

SSH Energy Bands - Eigenstates

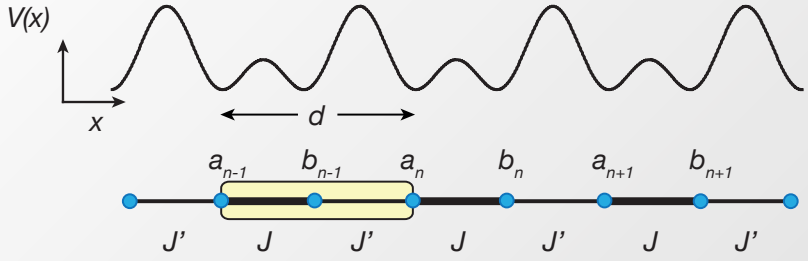

...ABABA... Lattice Structure....

$$\sum_x \Psi_x = \sum_x e^{ikx} \times \begin{cases} \alpha_k \\ \beta_k \; e^{ikd/2} \end{cases}$$

Berry Phase

SSH Energy Bands - Eigenstates

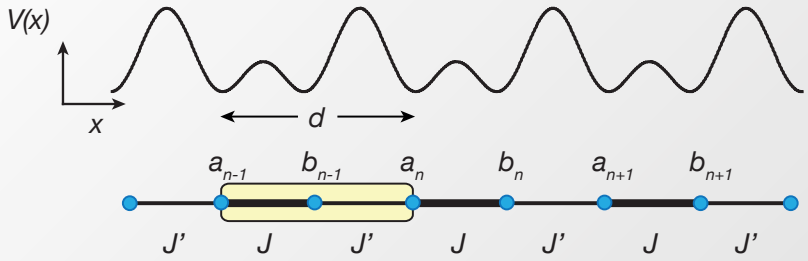

...ABABA... Lattice Structure....

$$\sum_x \Psi_x = \sum_x e^{ikx} \times \begin{cases} \alpha_k \\ \beta_k \; e^{ikd/2} \end{cases}$$

2x2 Hamiltonian:

$$\begin{bmatrix} 0 & -\rho_k \\ -\rho_k^* & 0 \end{bmatrix} \begin{pmatrix} \alpha_k \\ \beta_k \end{pmatrix} = \tilde{\epsilon}_k \begin{pmatrix} \alpha_k \\ \beta_k \end{pmatrix}$$

with $\rho_k = Je^{ikd/2} + J'e^{-ikd/2} = |\epsilon_k| e^{i\theta_k}$

SSH Energy Bands - Eigenstates

...ABABA... Lattice Structure....

$$\sum_x \Psi_x = \sum_x e^{ikx} \times \begin{cases} \alpha_k \\ \beta_k \; e^{ikd/2} \end{cases}$$

Eigenstates

$$\begin{pmatrix} \alpha_{k,\mp} \\ \beta_{k,\mp} \end{pmatrix} = \frac{1}{\sqrt{2}} \begin{pmatrix} \pm 1 \\ e^{-i\theta_k} \end{pmatrix}$$

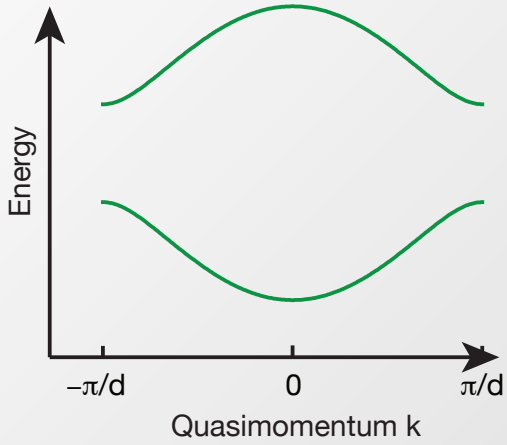

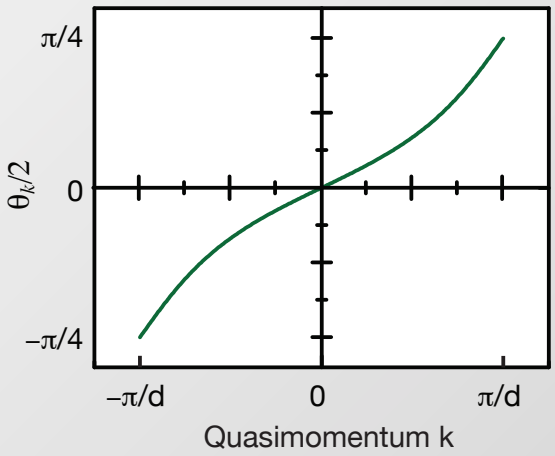

Berry Phase

SSH Energy Bands - Eigenstates

...ABABA... Lattice Structure....

$$\sum_x \Psi_x = \sum_x e^{ikx} \times \begin{cases} \alpha_k \\ \beta_k \; e^{ikd/2} \end{cases}$$

Eigenstates

$$\begin{pmatrix} \alpha_{k,\mp} \\ \beta_{k,\mp} \end{pmatrix} = \frac{1}{\sqrt{2}} \begin{pmatrix} \pm 1 \\ e^{-i\theta_k} \end{pmatrix}$$

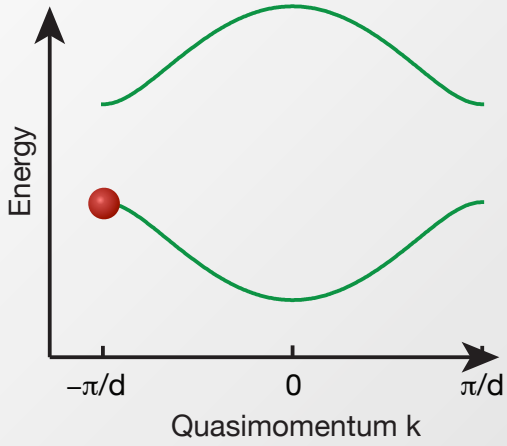

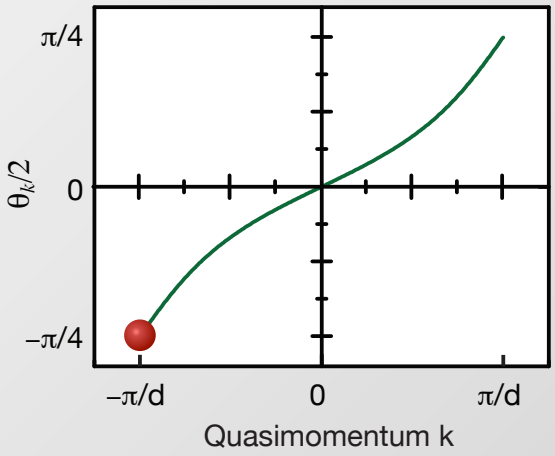

Adiabatic evolution in momentum space

SSH Energy Bands - Eigenstates

...ABABA... Lattice Structure....

$$\sum_x \Psi_x = \sum_x e^{ikx} \times \begin{cases} \alpha_k \\ \beta_k \; e^{ikd/2} \end{cases}$$

Eigenstates

$$\begin{pmatrix} \alpha_{k,\mp} \\ \beta_{k,\mp} \end{pmatrix} = \frac{1}{\sqrt{2}} \begin{pmatrix} \pm 1 \\ e^{-i\theta_k} \end{pmatrix}$$

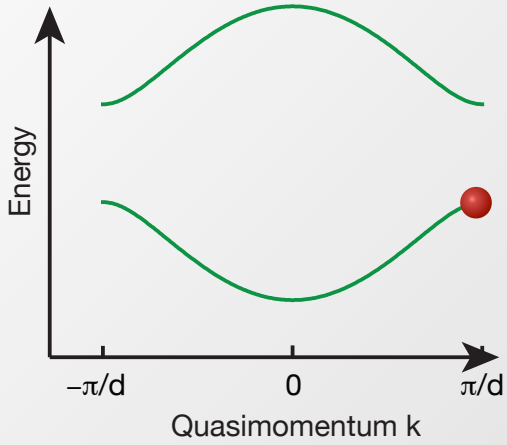

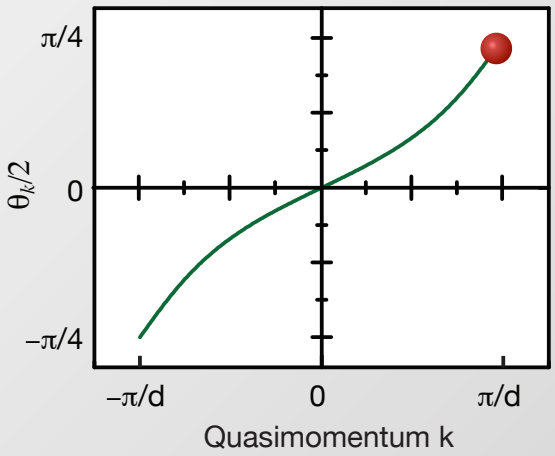

Adiabatic evolution in momentum space

Berry Phase

SSH Energy Bands - Eigenstates

...ABABA... Lattice Structure....

$$\sum_x \Psi_x = \sum_x e^{ikx} \times \begin{cases} \alpha_k \\ \beta_k \; e^{ikd/2} \end{cases}$$

Eigenstates

$$\begin{pmatrix} \alpha_{k,\mp} \\ \beta_{k,\mp} \end{pmatrix} = \frac{1}{\sqrt{2}} \begin{pmatrix} \pm 1 \\ e^{-i\theta_k} \end{pmatrix}$$

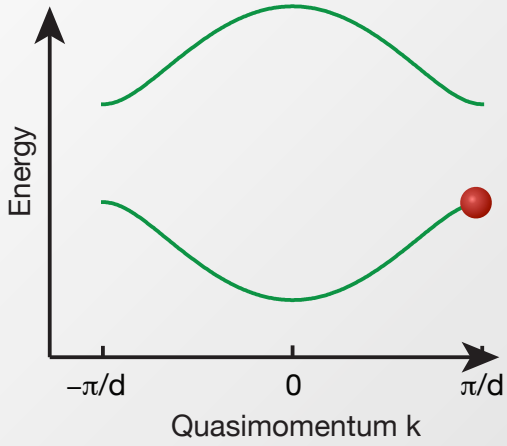

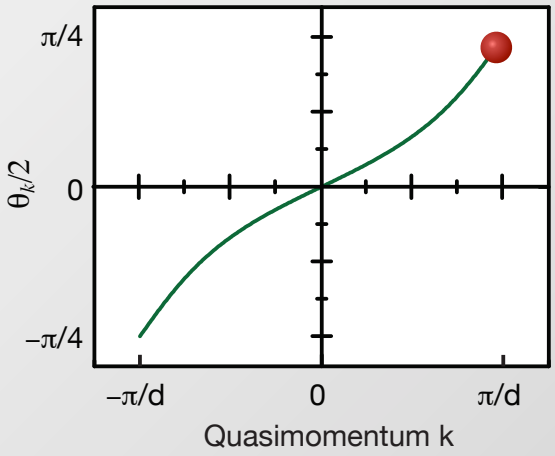

$$\varphi_{Zak} = i \int_{k_0}^{k_0+G} \left(\alpha_k^* \partial_k \alpha_k + \beta_k^* \partial_k \beta_k\right) \; dk$$

Zak Phase
SSH Model

SSH Energy Bands - Eigenstates

...ABABA... Lattice Structure....

$$\sum_x \Psi_x = \sum_x e^{ikx} \times \begin{cases} \alpha_k \\ \beta_k \; e^{ikd/2} \end{cases}$$

Eigenstates

$$\begin{pmatrix} \alpha_{k,\mp} \\ \beta_{k,\mp} \end{pmatrix} = \frac{1}{\sqrt{2}} \begin{pmatrix} \pm 1 \\ e^{-i\theta_k} \end{pmatrix}$$

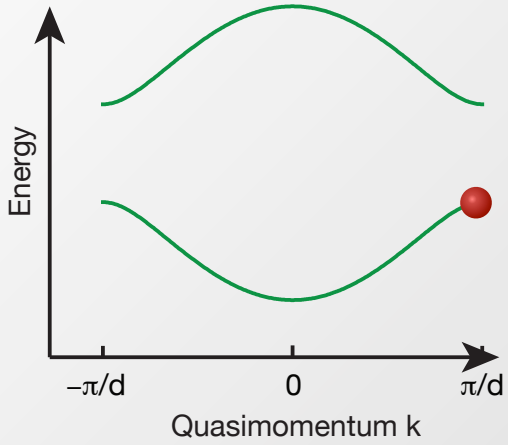

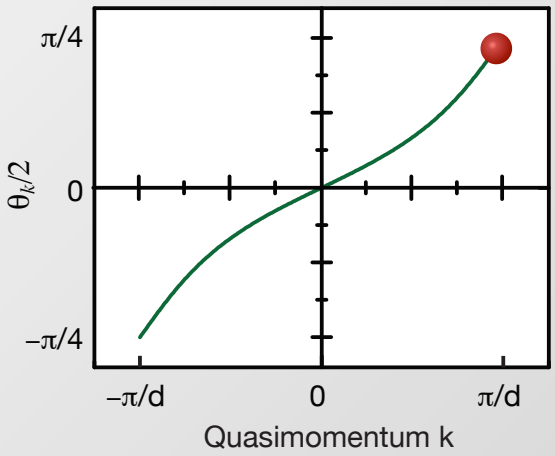

$$\varphi_{Zak} = \frac{1}{2} \int_{k_0}^{G+k_0} \partial_k \theta_k \; dk$$

Berry Phase

SSH Energy Bands - Eigenstates

...ABABA... Lattice Structure....

$$\sum_x \Psi_x = \sum_x e^{ikx} \times \begin{cases} \alpha_k \\ \beta_k \; e^{ikd/2} \end{cases}$$

Eigenstates

$$\begin{pmatrix} \alpha_{k,\mp} \\ \beta_{k,\mp} \end{pmatrix} = \frac{1}{\sqrt{2}} \begin{pmatrix} \pm 1 \\ e^{-i\theta_k} \end{pmatrix}$$

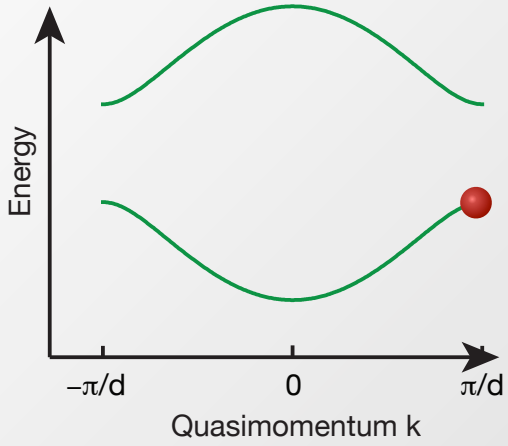

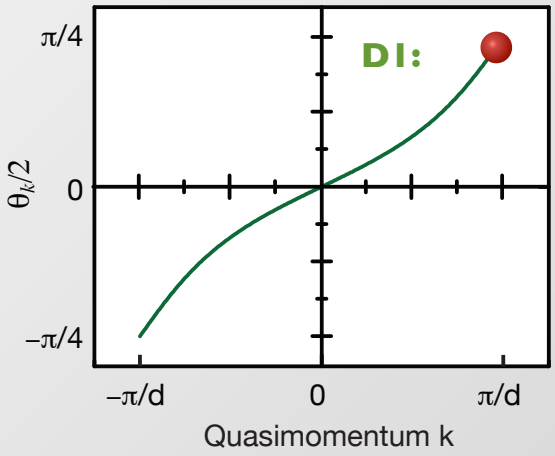

DI: $J > J'$ $\quad \varphi_{Zak}^{D1} = \frac{\pi}{2}$

SSH Energy Bands - Eigenstates

...ABABA... Lattice Structure....

$$\sum_x \Psi_x = \sum_x e^{ikx} \times \begin{cases} \alpha_k \\ \beta_k \; e^{ikd/2} \end{cases}$$

Eigenstates

$$\begin{pmatrix} \alpha_{k,\mp} \\ \beta_{k,\mp} \end{pmatrix} = \frac{1}{\sqrt{2}} \begin{pmatrix} \pm 1 \\ e^{-i\theta_k} \end{pmatrix}$$

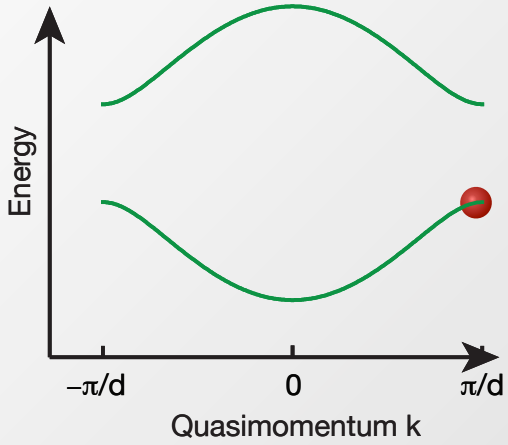

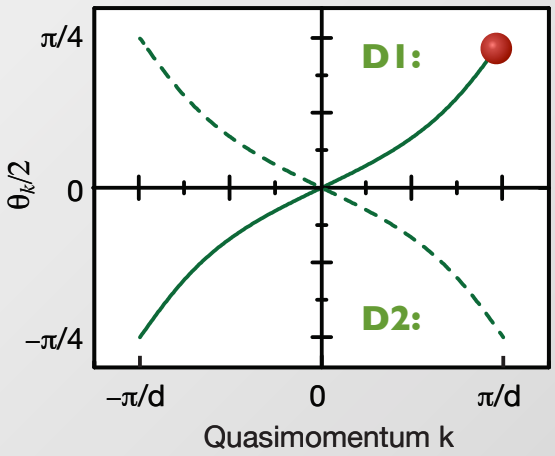

D1: $J > J'$ $\quad \varphi_{Zak}^{D1} = \frac{\pi}{2}$

D2: $J' > J$ $\quad \varphi_{Zak}^{D2} = -\frac{\pi}{2}$

Realization with ultracold atoms

$$H_{\mathrm{SSH}} = -\sum_n \left\{ J a_n^\dagger b_n + J' a_n^\dagger b_{n-1} + \mathrm{h.c.} \right\}$$

767 nm
1534 nm

D1: $J > J'$

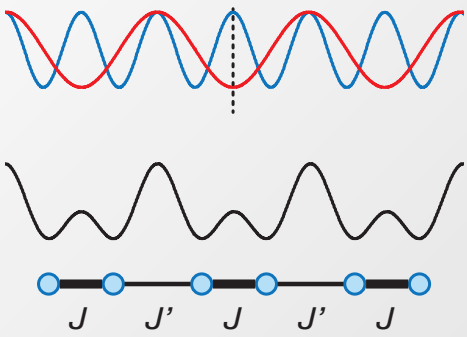

D2: $J' > J$

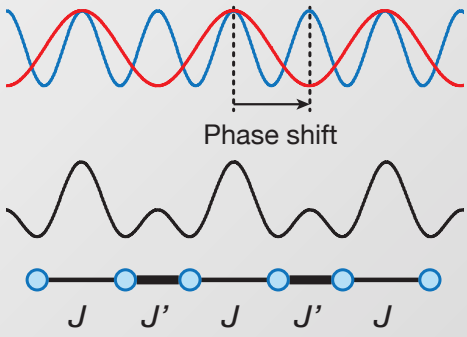

$$\delta\varphi_{Zak} = \varphi_{Zak}^{D1} - \varphi_{Zak}^{D2} = \pi$$

Measuring the Berry-Zak Phase (SSH Model)

DI: $J > J'$ Spin-dependent Bloch oscillations + Ramsey interferometry

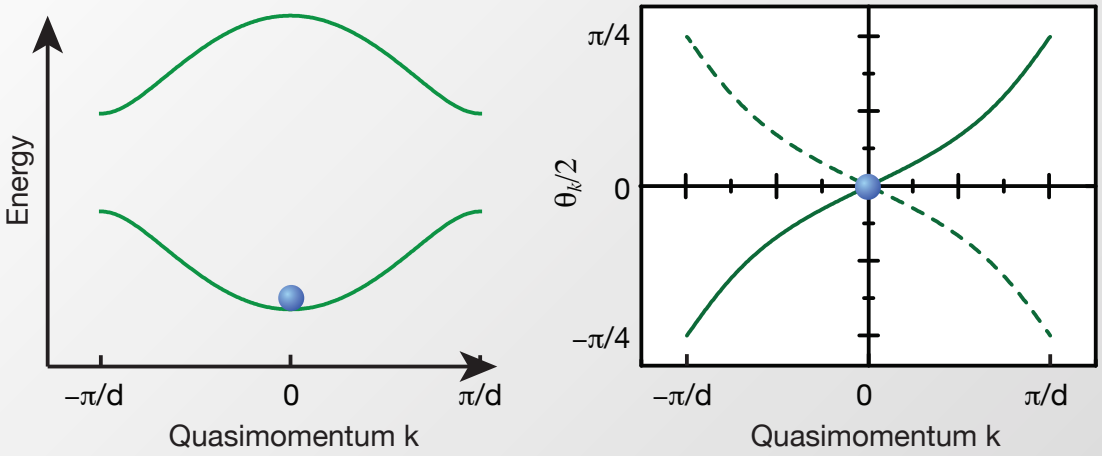

Prepare BEC in state $|\sigma, k\rangle = |\downarrow, 0\rangle\,, \quad \text{with } \sigma = \uparrow, \downarrow$

Measuring the Berry-Zak Phase (SSH Model)

DI: $J > J'$

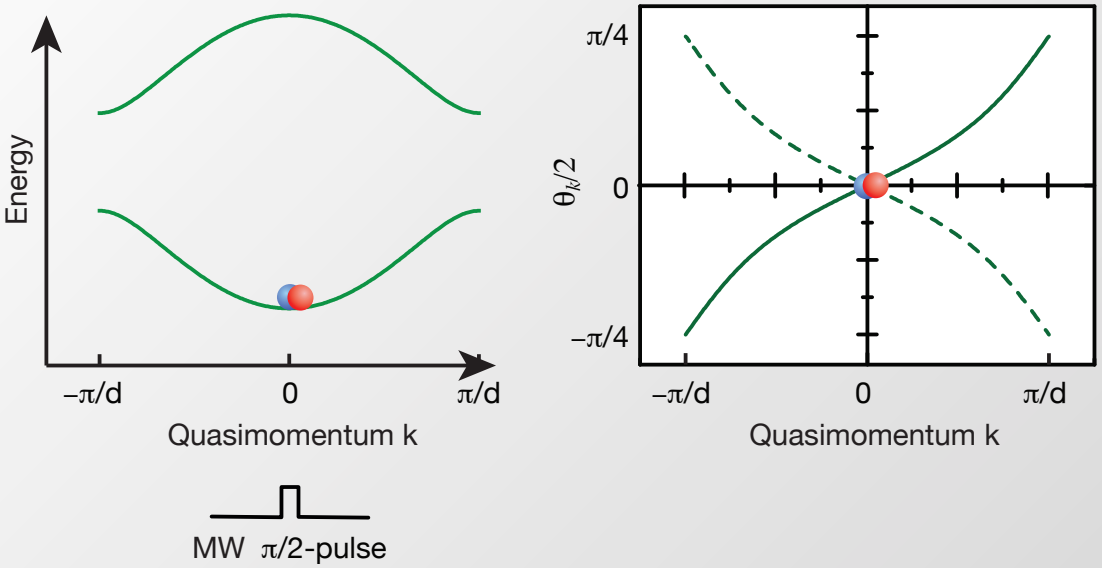

Create coherent superposition $\frac{1}{\sqrt{2}}\left(|\uparrow, 0\rangle + |\downarrow, 0\rangle\right)$

Measuring the Berry-Zak Phase (SSH Model)

DI: $J > J'$

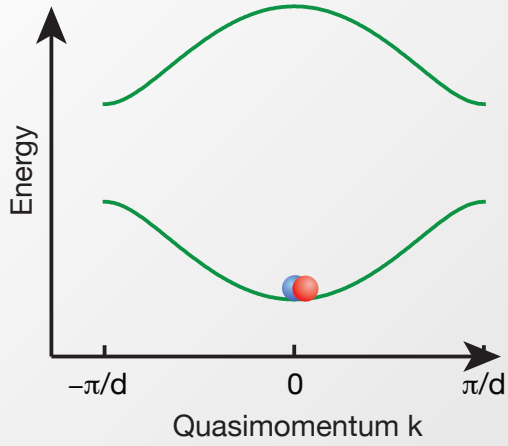

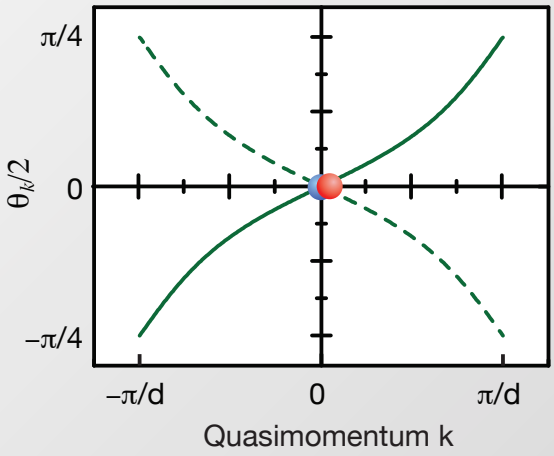

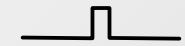

MW π/2-pulse

Spin components with opposite magnetic moments!

Create coherent superposition $\frac{1}{\sqrt{2}}\left(|\uparrow,0\rangle + |\downarrow,0\rangle\right)$

Berry Phase

Measuring the Berry-Zak Phase (SSH Model)

DI: $J > J'$

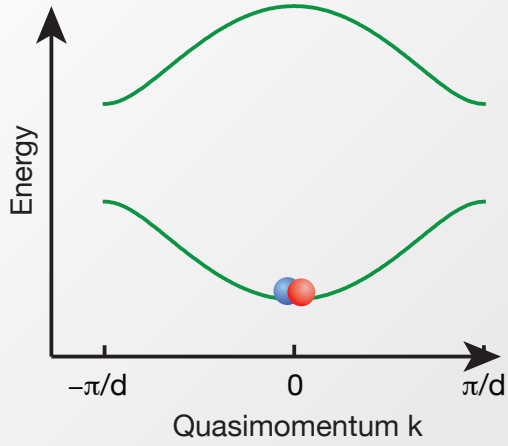

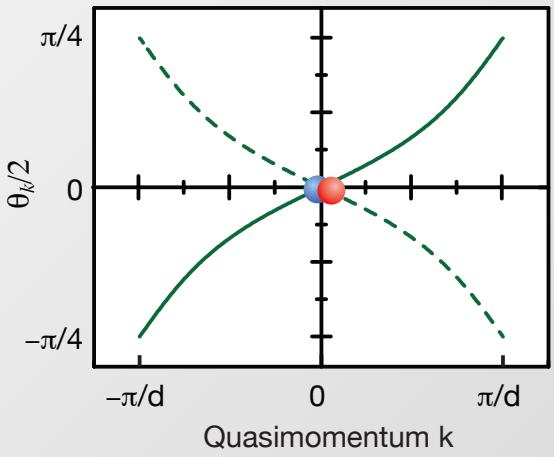

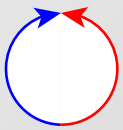

Closed Loop in *k*-Space

Apply magnetic field gradient $\rightarrow$ adiabatic evolution in momentum space

Measuring the Berry-Zak Phase (SSH Model)

DI: $J > J'$

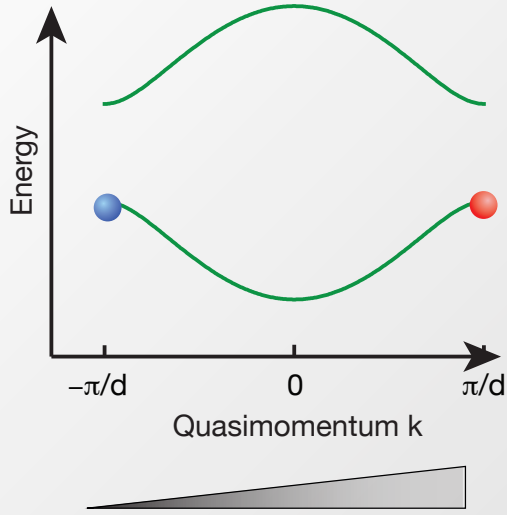

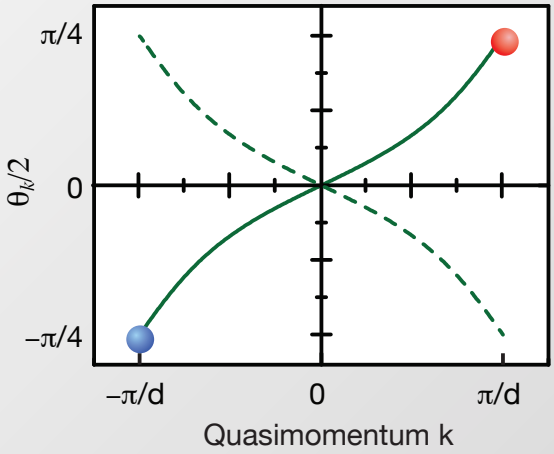

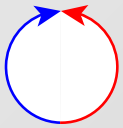

Closed Loop in *k*-Space

Apply magnetic field gradient $\rightarrow$ adiabatic evolution in momentum space

Berry Phase

Measuring the Berry-Zak Phase (SSH Model)

DI: $J > J'$

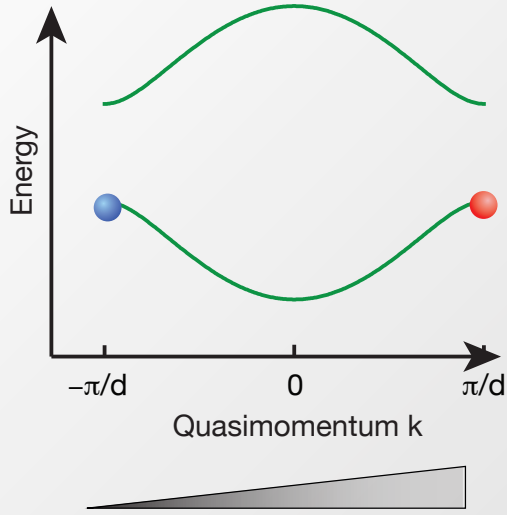

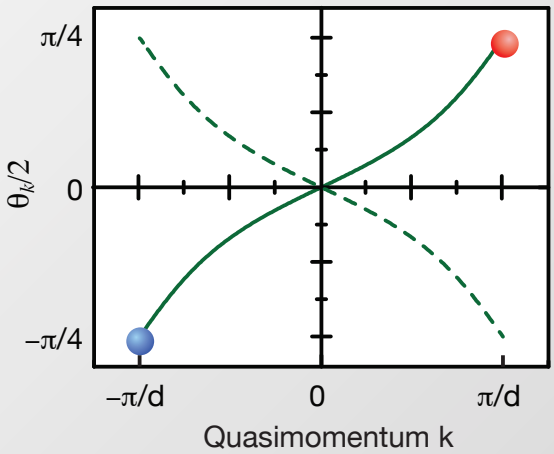

$$\delta\varphi_{Zak} = \varphi_{Zak}^{D1} + \varphi_{dyn} + \varphi_{Zeeman}$$

Measuring the Berry-Zak Phase (SSH Model)

D1: $J > J'$

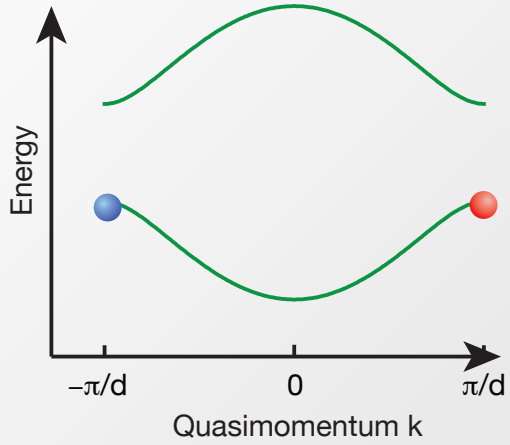

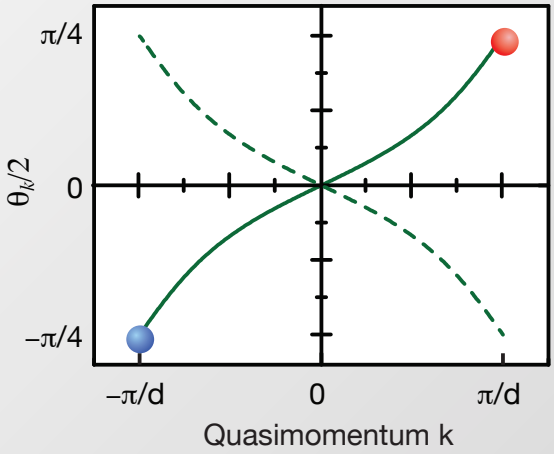

$$\varphi_{dyn} = \int E(t)/\hbar \; \mathrm{dt}$$

$$E(k) = E(-k)$$

$$\delta\varphi_{Zak} = \varphi_{Zak}^{D1} + \varphi_{dyn} + \varphi_{Zeeman}$$

Measuring the Berry-Zak Phase (SSH Model)

D1: $J > J'$ → **D2:** $J' > J$

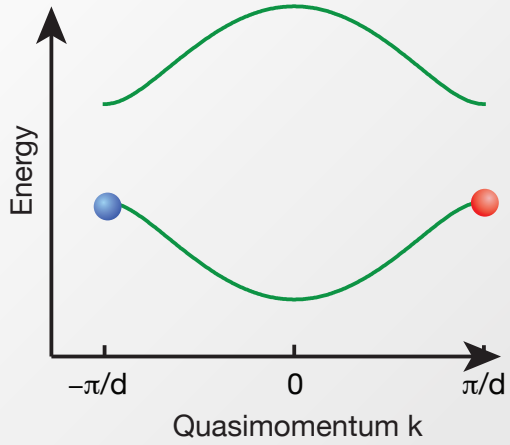

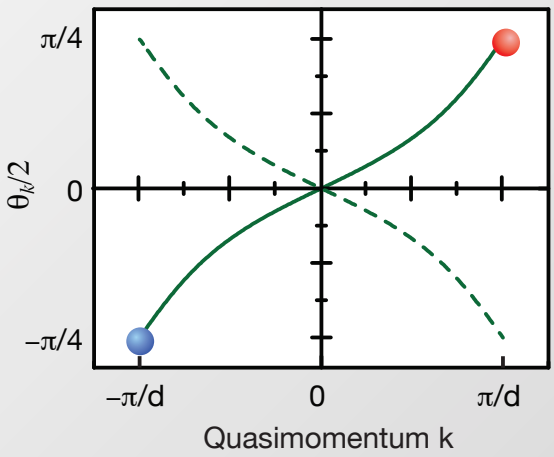

MW π-pulse

Apply Spin-Echo pulse + dimerization change

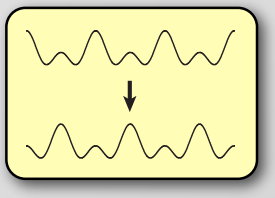

Measuring the Berry-Zak Phase (SSH Model)

D1: $J > J'$ → **D2:** $J' > J$

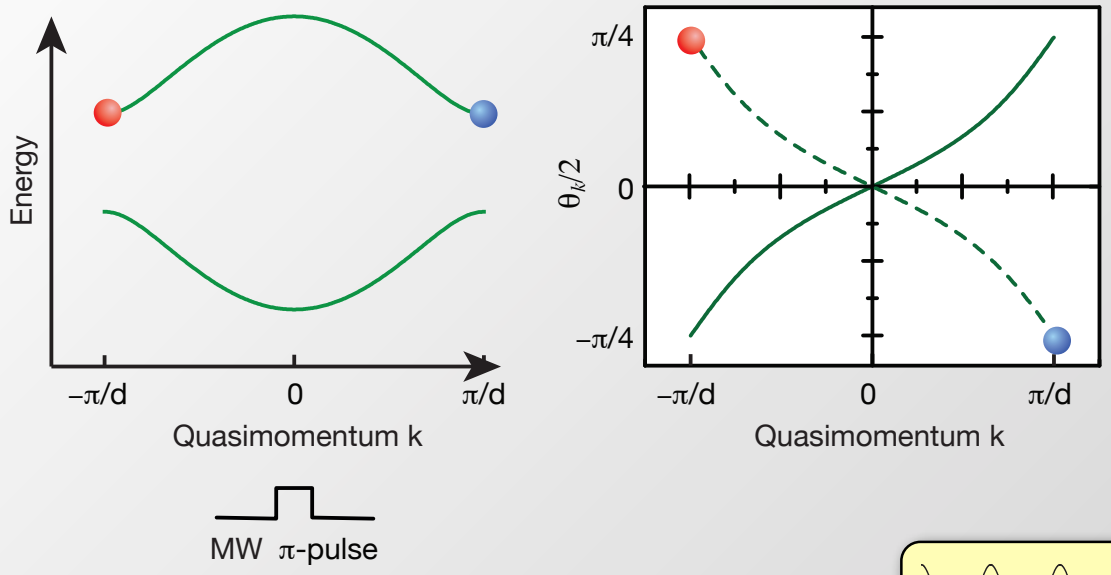

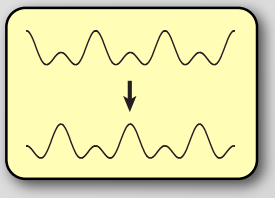

Apply Spin-Echo pulse + dimerization change

Measuring the Berry-Zak Phase (SSH Model)

D2: $J' > J$

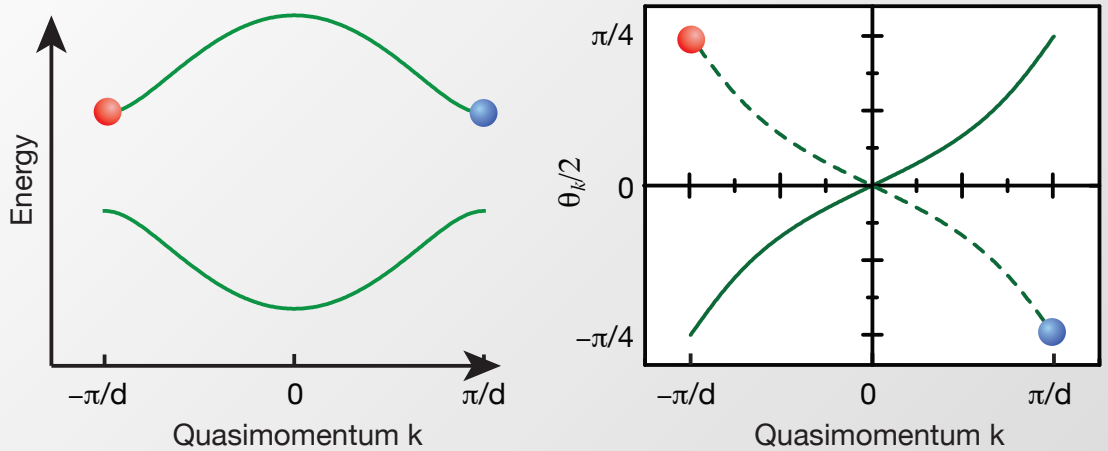

Apply magnetic field gradient → adiabatic evolution in momentum space

Measuring the Berry-Zak Phase (SSH Model)

D2: $J' > J$

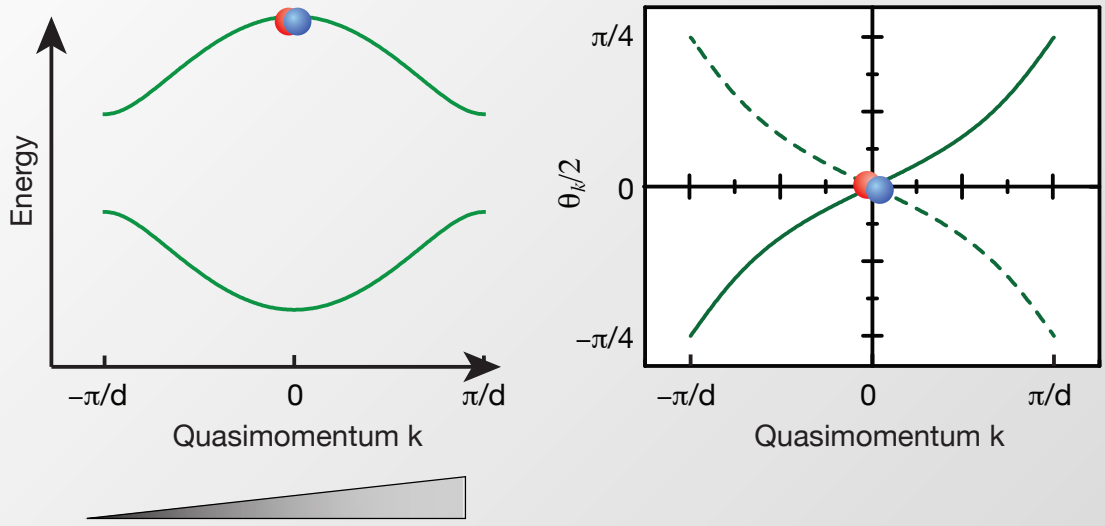

Apply magnetic field gradient $\rightarrow$ adiabatic evolution in momentum space

Berry Phase

Measuring the Berry-Zak Phase (SSH Model)

D2: $J' > J$

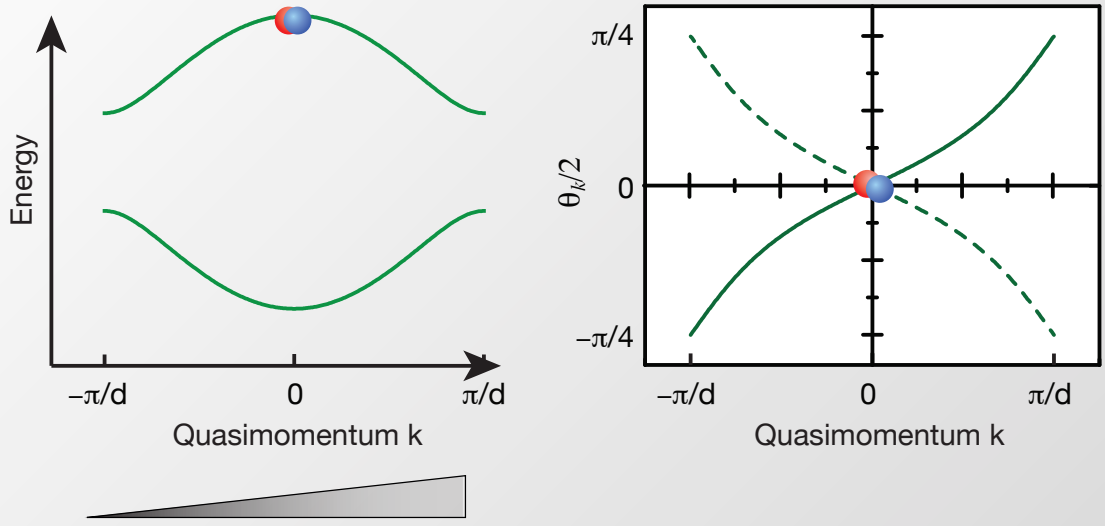

$$\delta\varphi_{Zak} = \varphi_{Zak}^{D1} - \varphi_{Zak}^{D2} + \varphi_{Zeeman}$$

Measuring the Berry-Zak Phase (SSH Model)

D2: $J' > J$

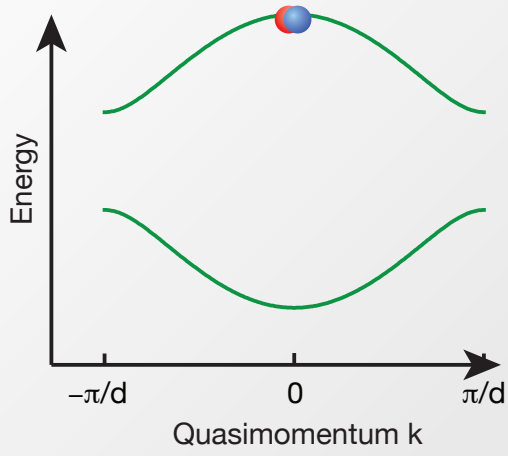

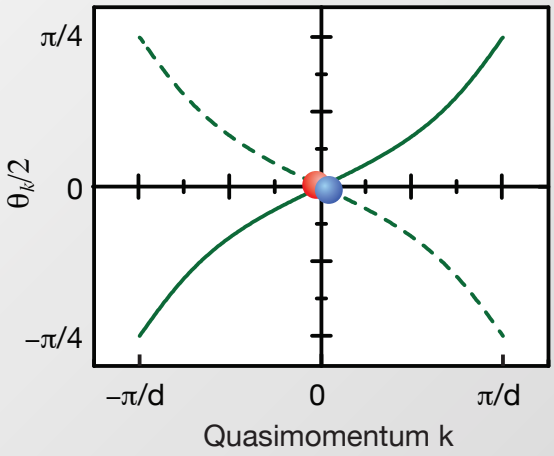

Spin-Echo pulse

$$\delta\varphi_{Zak} = \varphi_{Zak}^{D1} - \varphi_{Zak}^{D2} + \varphi_{Zeeman}$$

Berry Phase

Measuring the Berry-Zak Phase (SSH Model)

D2: $J' > J$

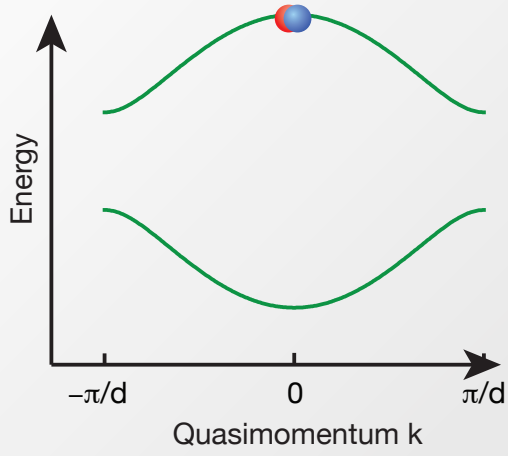

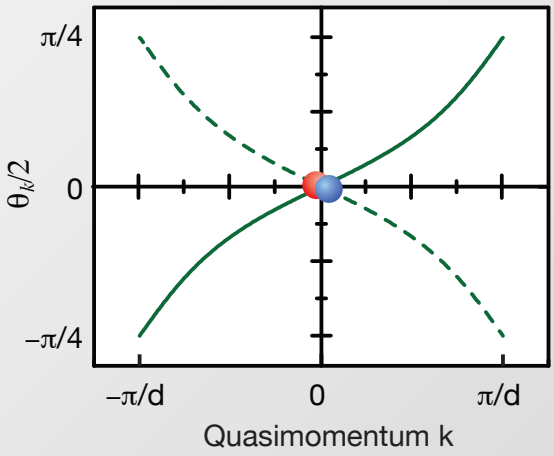

MW π/2-pulse, with phase φ_{MW}

Detect phase difference
with Ramsey interferometry

$$\delta\varphi_{Zak} = \varphi_{Zak}^{D1} - \varphi_{Zak}^{D2}$$

Reference measurement

Phase of reference fringe:

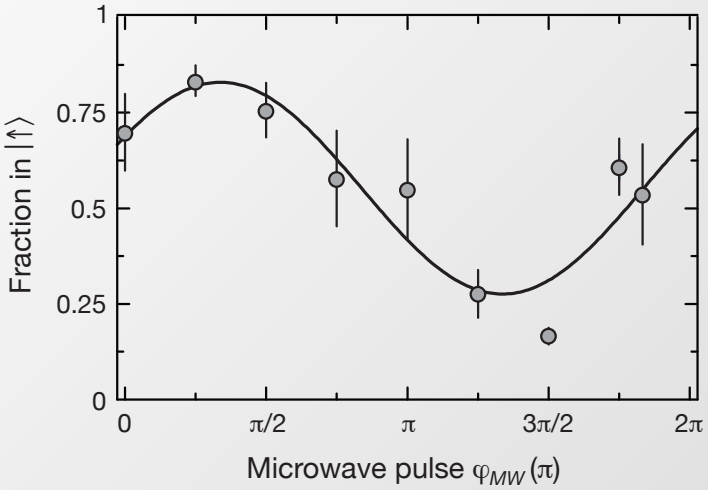

$\delta\varphi \neq 0$

Average of five individual measurements

Exp. imperfections: - Small detuning of the MW-pulse
- Magnetic field drifts

Measuring the Zak Phase (SSH Model)

Measured Topological invariant:
Zak phase difference

$$\varphi_{Zak}^{D1} - \varphi_{Zak}^{D2} = \pi$$

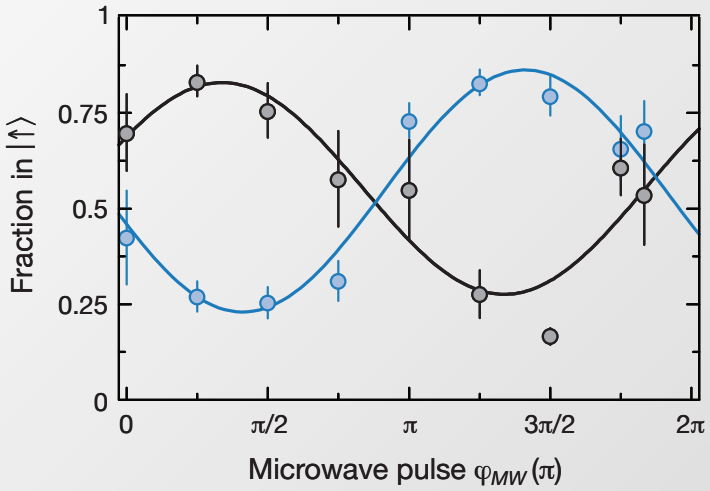

$\delta\varphi_{Zak} = 0.97(2)\pi$

obtained from 14
independent measurements

Measuring the Zak Phase (SSH Model)

Measured Topological invariant: Zak phase difference

$$\varphi_{Zak}^{D1} - \varphi_{Zak}^{D2} = \pi$$

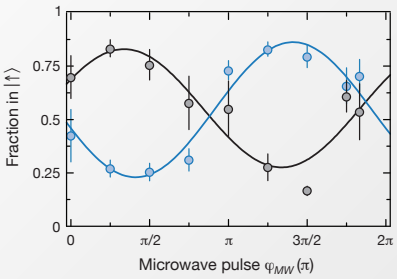

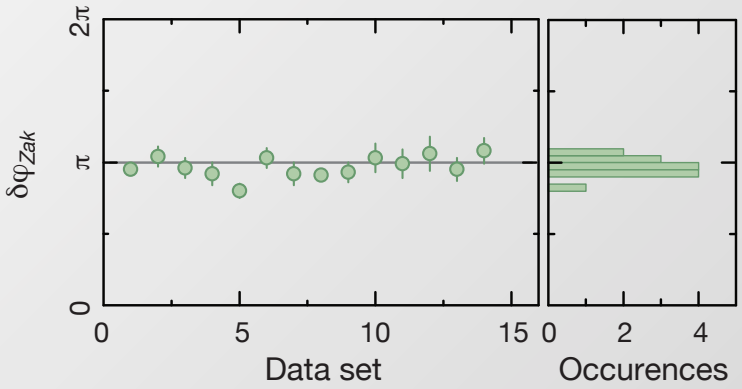

$$\delta\varphi_{Zak} = 0.97(2)\pi$$

obtained from 14 independent measurements

Fractional Zak Phase

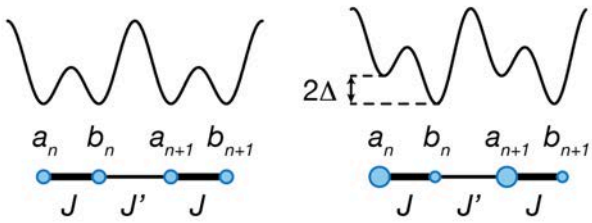

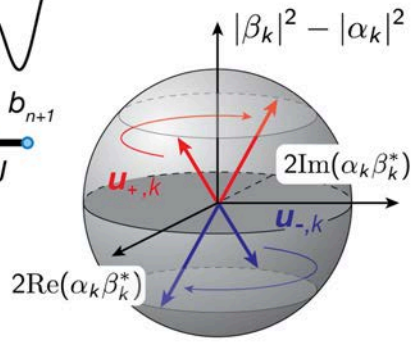

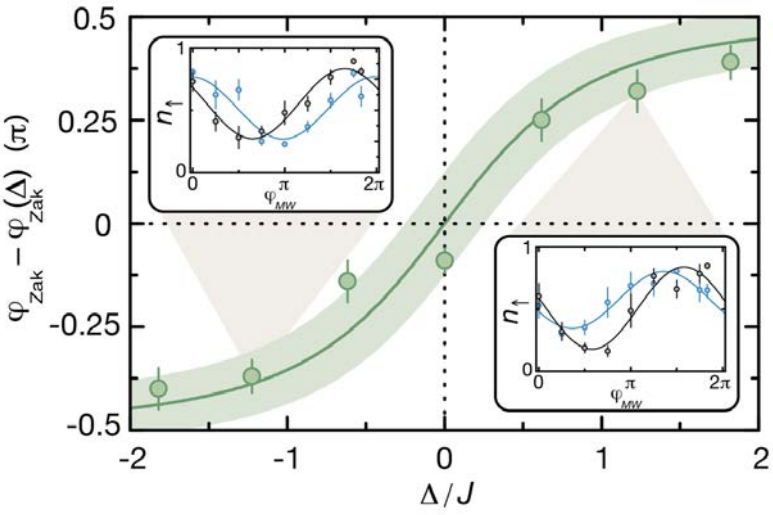

Zak Phase becomes **fractional** for heteropolar dimerization!

Measuring Fractional Charge

Probability Density of Eigenstates

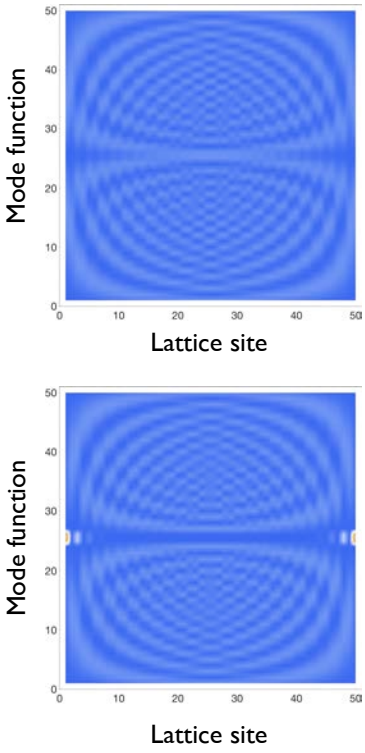

Lattice Topology

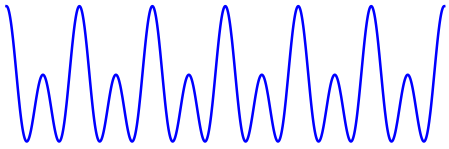

Topologically Trivial

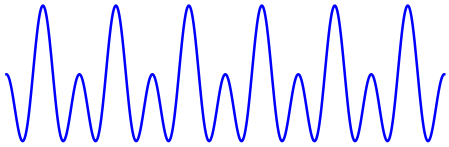

Topologically Non-Trivial

Fractional Charge

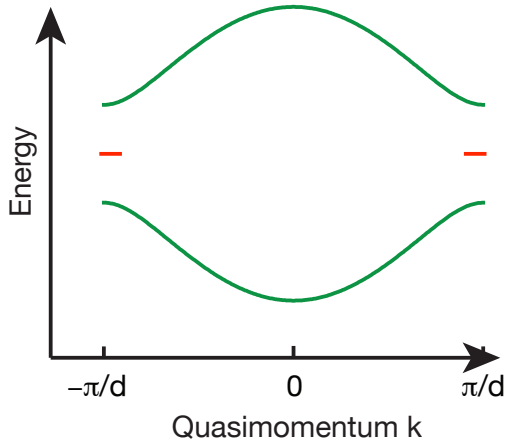

R. Rajaraman & J. Bell, Phys. Lett B 1982, Nucl. Phys. B 1983

Fractional Charge

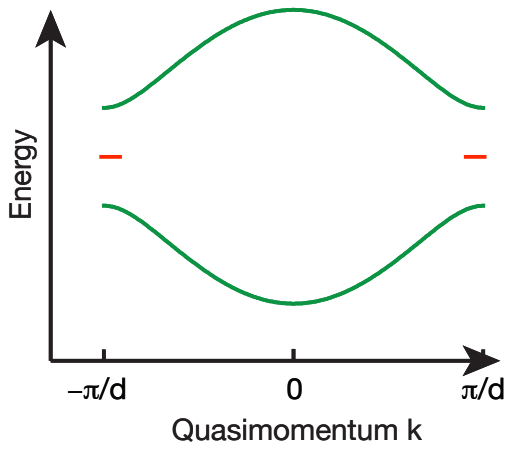

R. Rajaraman & J. Bell, Phys. Lett B 1982, Nucl. Phys. B 1983

SSH

Fractional Charge

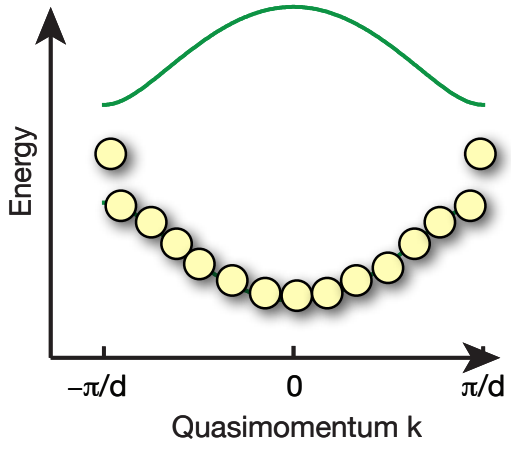

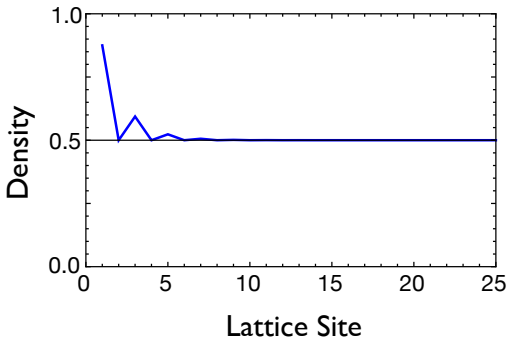

R. Rajaraman & J. Bell, Phys. Lett B 1982, Nucl. Phys. B 1983

Fractional Charge

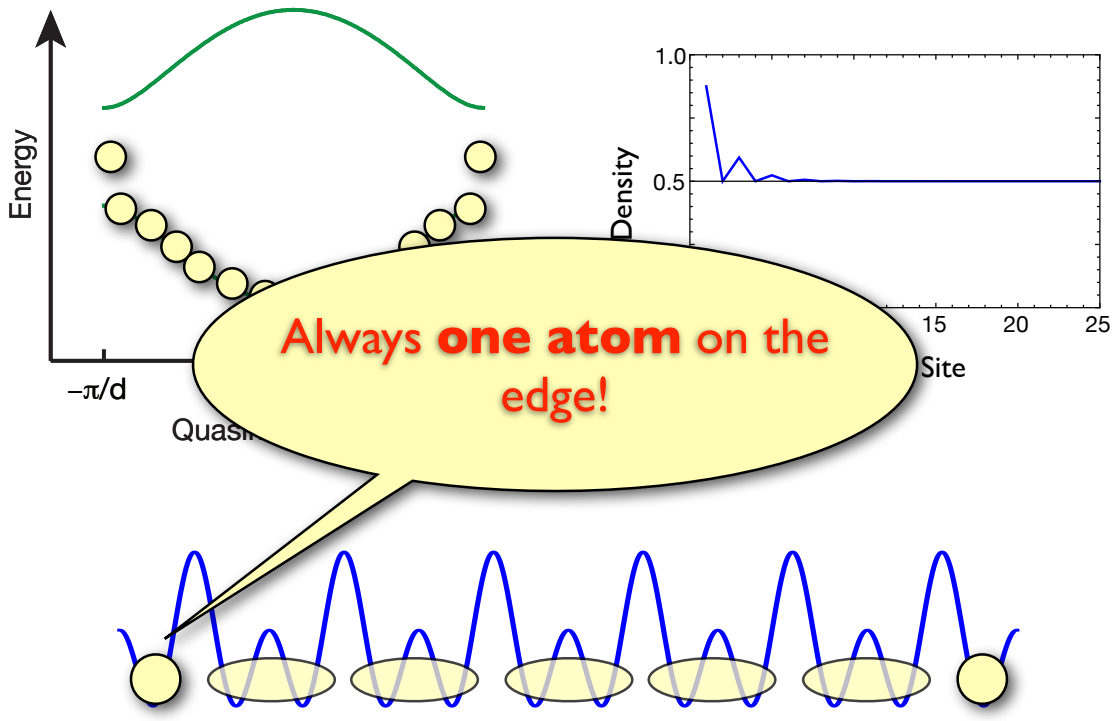

R. Rajaraman & J. Bell, Phys. Lett B 1982, Nucl. Phys. B 1983

'Aharonov-Bohm' Interferometer for Measuring Berry Curvature

Hexagonal Lattices

Lattice: A and B degenerate sublattices

$$H = H_0 - J\sum_{\mathbf{R}}\sum_{i=1}^{3}\left(\hat{a}_{\mathbf{R}}\hat{b}^{\dagger}_{\mathbf{R}+\mathbf{d}_i} + \text{h.c.}\right)$$

Real Space

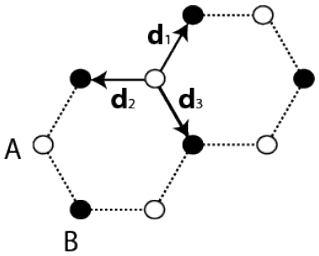

Lowest energy bands:

Dirac points at the corners of the first BZ

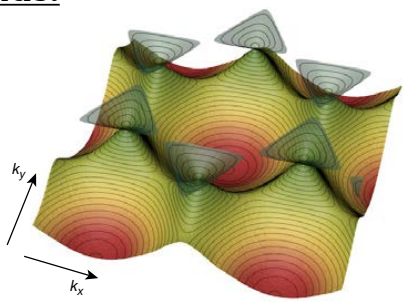

Reciprocal Space

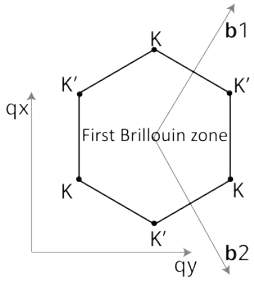

A. Castro Neto et al., Rev. Mod. Phys. **81**, 109 (2009)
cold atoms: hexagonal - K. Sengtsock (Hamburg), brick wall - T. Esslinger (Zürich)

Scalar & Geometric Features

Band structure characterized by **scalar** & **geometric** features!

Eigenstates: Bloch waves $\psi_{\mathbf{q},n}(\mathbf{r}) = e^{i\mathbf{q}\mathbf{r}}u_{\mathbf{q},n}(\mathbf{r})$

Scalar Features

Dispersion relation

$E_{\mathbf{q},n}$

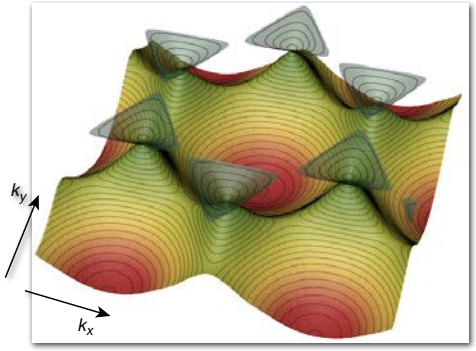

Geometric Features

Berry connection

$\mathbf{A}_n(\mathbf{q}) = i\langle u_{\mathbf{q},n}|\nabla_{\mathbf{q}}|u_{\mathbf{q},n}\rangle$

Berry curvature

$\Omega_n(\mathbf{q}) = \nabla_{\mathbf{q}} \times \mathbf{A}_{\mathbf{n}}(\mathbf{q}) \cdot \mathbf{e}_z$

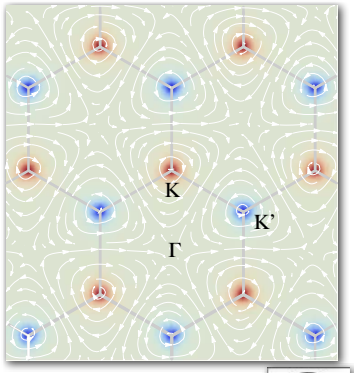

'Aharonov Bohm' Interferometer in Momentum Space

Real Space

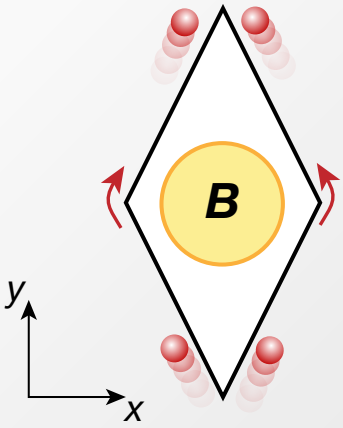

$$\varphi_{AB} = \frac{q}{\hbar}\oint_C \mathbf{A}(\mathbf{r})\,d\mathbf{r} = \frac{q}{\hbar}\int_S \nabla\times\mathbf{A}(\mathbf{r})\,d^2r$$

$$\varphi_{AB} = \frac{q}{\hbar}\int \mathbf{B}\,d\mathbf{S} = 2\pi\Phi/\Phi_0$$

Aharonov-Bohm Phase

'Aharonov Bohm' Interferometer in Momentum Space

Real Space

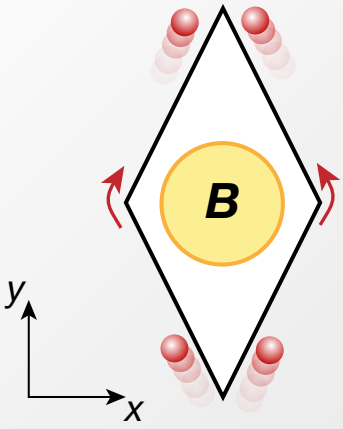

Momentum Space

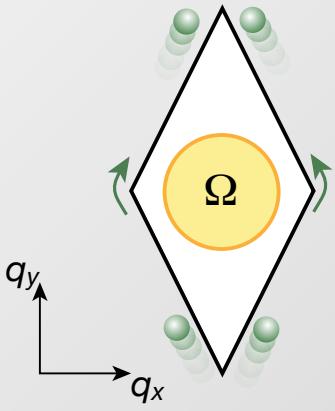

$$\varphi_{AB} = \frac{q}{\hbar}\oint_C \mathbf{A}(\mathbf{r})\,d\mathbf{r} = \frac{q}{\hbar}\int_S \nabla\times\mathbf{A}(\mathbf{r})\,d^2r$$

$$\varphi_{AB} = \frac{q}{\hbar}\int \mathbf{B}\,d\mathbf{S} = 2\pi\Phi/\Phi_0$$

Aharonov-Bohm Phase

$$\varphi_{\text{Berry}} = \oint_C \mathbf{A}_n(\mathbf{q})\,d\mathbf{q} = \int_{S_q} \nabla\times\mathbf{A}_n(\mathbf{r})\,d\mathbf{S}_q$$

$$\varphi_{\text{Berry}} = \int \Omega_n(\mathbf{q})\,d\mathbf{S}_q$$

Berry Phase

Berry Curvature in Hexagonal Lattices

Berry curvature **concentrated to Dirac cones, alternating in sign**!
Breaking time reversal or inversion symmetry gaps Dirac cones
and spreads Berry curvature out

Hexagonal Lattice Hamiltonian

$$H(\mathbf{q}) = \begin{pmatrix} \Delta & f(\mathbf{q}) \\ f(\mathbf{q}) & -\Delta \end{pmatrix}$$

Expanding momenta close to K Dirac point

$$H(\tilde{\mathbf{q}}) = \begin{pmatrix} 0 & \tilde{q}_x + i\tilde{q}_y \\ \tilde{q}_x - i\tilde{q}_y & 0 \end{pmatrix}$$

Eigenstates

$$u^{\pm}_{\mathbf{K},\tilde{\mathbf{q}}} = \frac{1}{2}\left(e^{i\theta(\mathbf{q})/2} \pm e^{-i\theta(\mathbf{q})/2}\right)$$

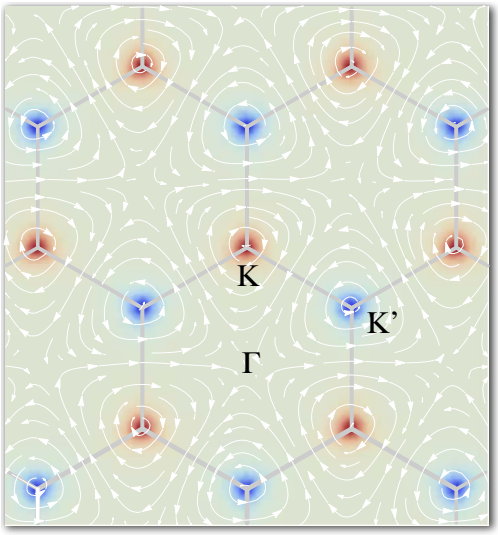

Berry Phases in Graphene

Berry Phase around K-Dirac cone

$$\varphi_{\text{Berry},\mathbf{K}} = \oint_C \mathbf{A}(\mathbf{q})\, d\mathbf{q} = \pi$$

Berry Phase around K'-Dirac cone

$$\varphi_{\text{Berry},\mathbf{K}'} = -\pi$$

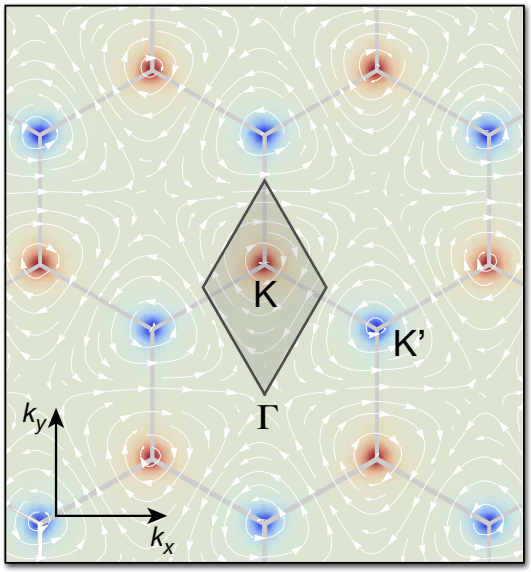

The Interferometer

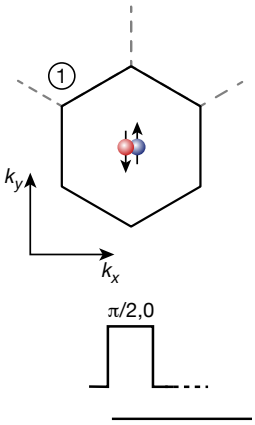

Forces applied by **lattice acceleration** and **magnetic gradients**!

Band Topology

The Interferometer

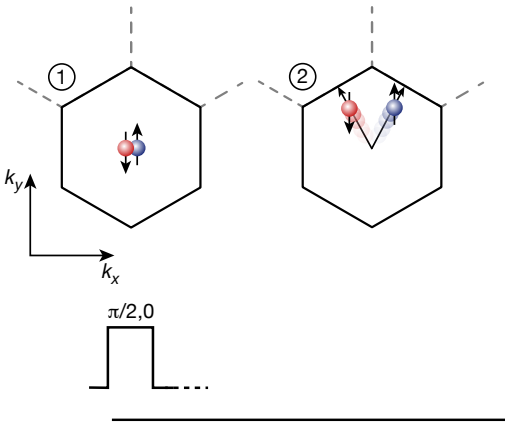

Forces applied by **lattice acceleration** and **magnetic gradients**!

The Interferometer

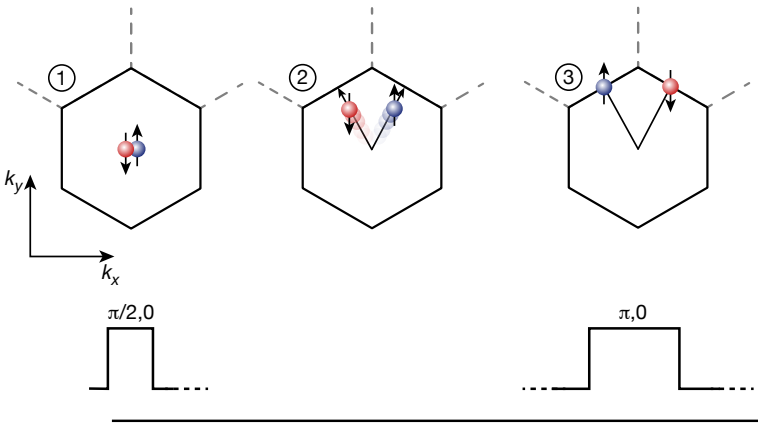

Forces applied by **lattice acceleration** and **magnetic gradients**!

Band Topology

The Interferometer

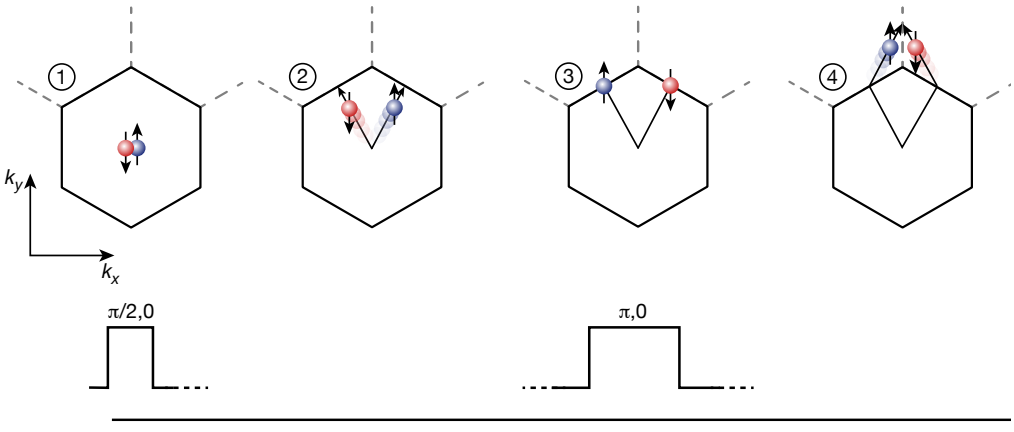

Forces applied by **lattice acceleration** and **magnetic gradients**!

The Interferometer

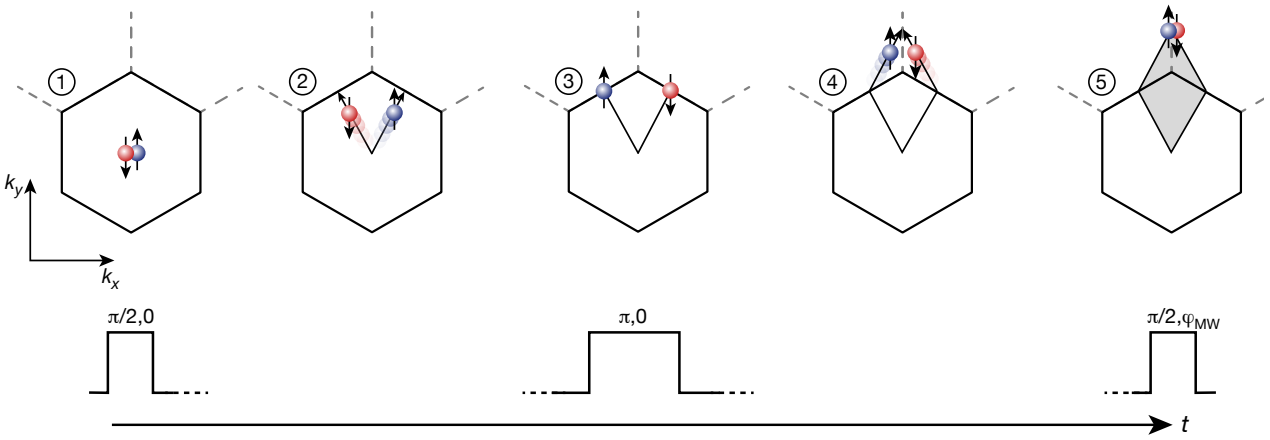

Forces applied by **lattice acceleration** and **magnetic gradients**!

Interferometry Results

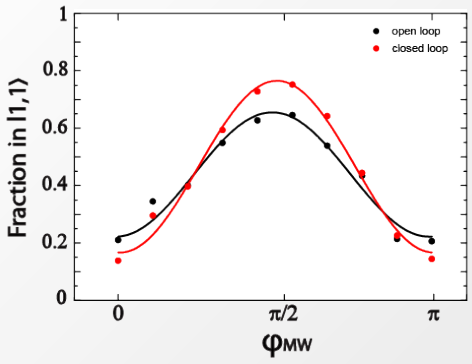

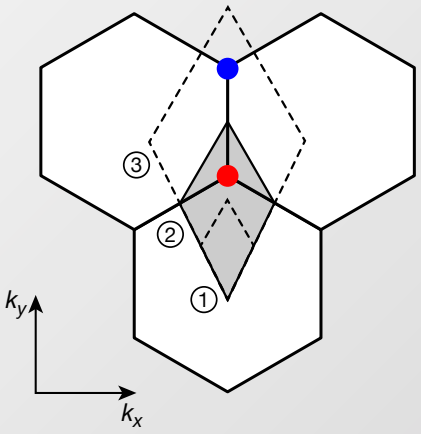

Interferometry Results

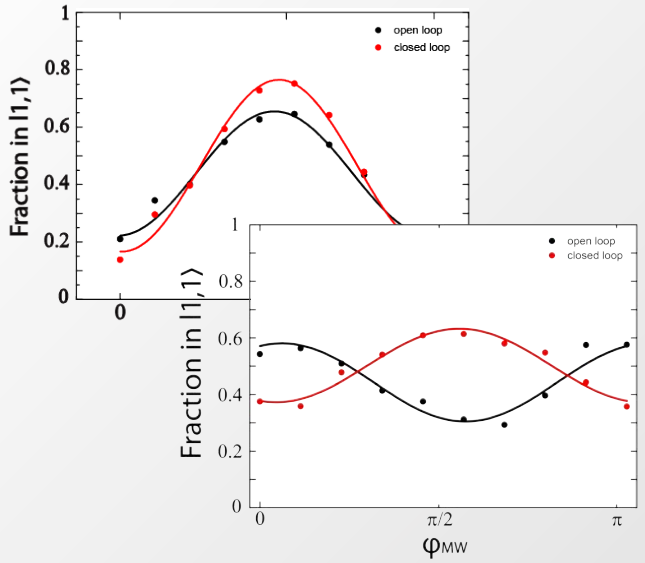

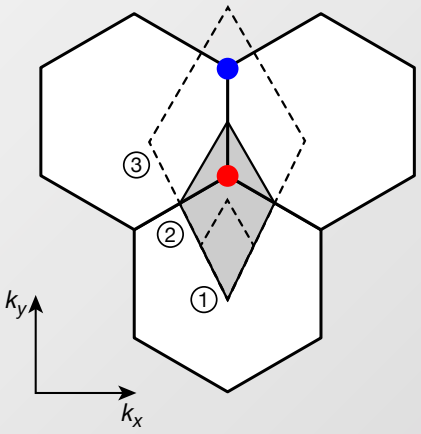

Band Topology

Interferometry Results

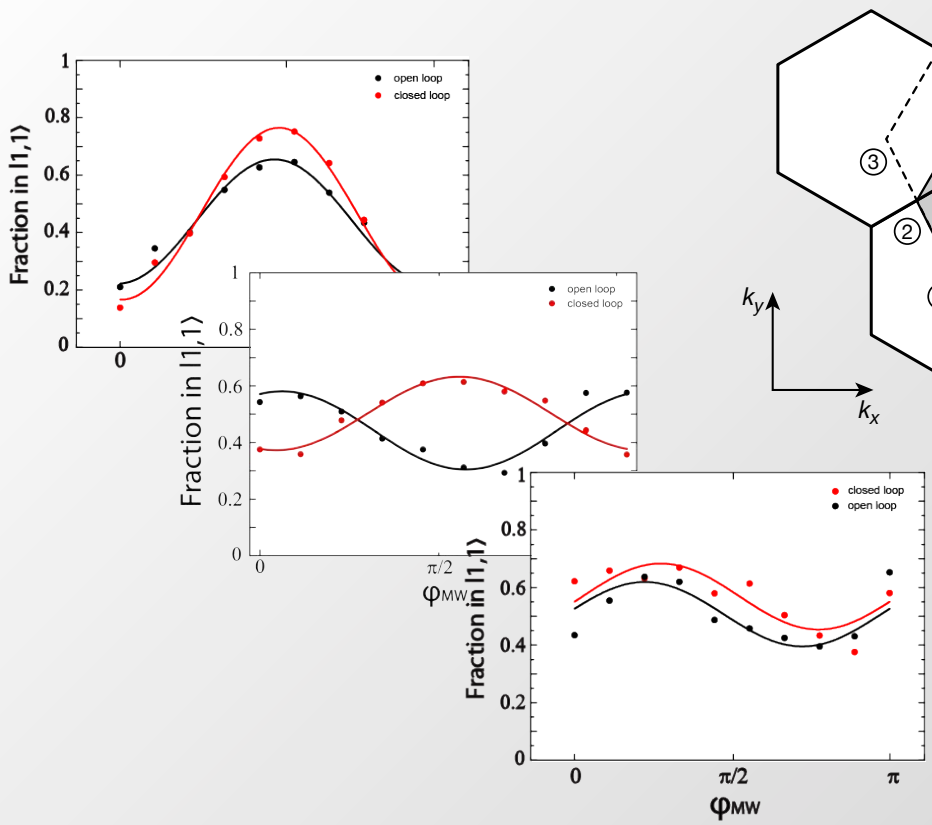

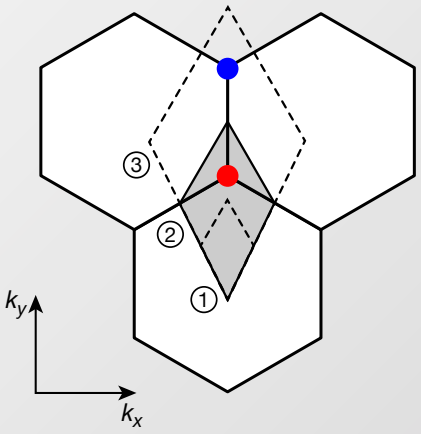

Stückelberg Interferometry

Lattice acceleration allows for arbitrary path choice

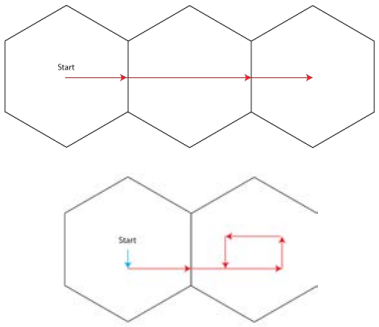

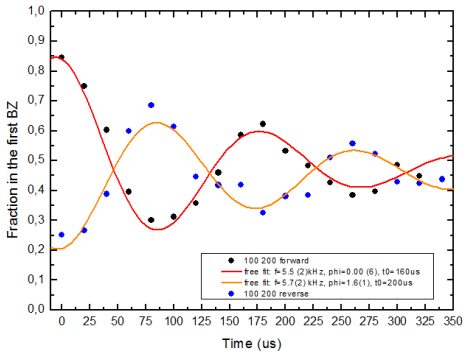

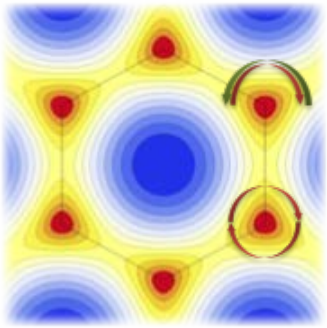

Has allowed us to detect
off-diagonal Berry connection through Wilson loops!

Outlook

- Rectified Flux, Hofstadter Butterfly
- Novel Correlated Phases in Strong Fields, Transport Measurements
- Adiabatic loading schemes
- Spectroscopy of Hoftstadter bands
- Novel Topological Insulators
- Image Edge States - directly/spectroscopically
- Measure spatially resolved full current distribution
- Non-equilibrium dynamics in gauge fields
- Thermalization?

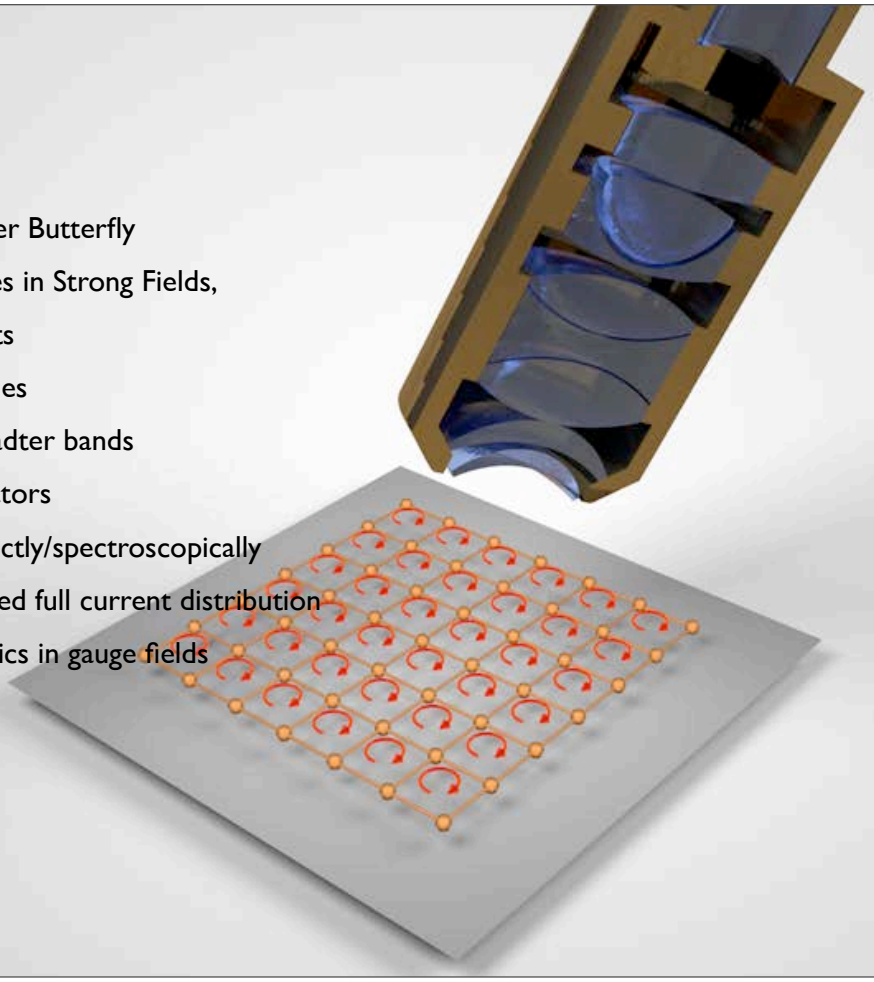

Gauge Field Team

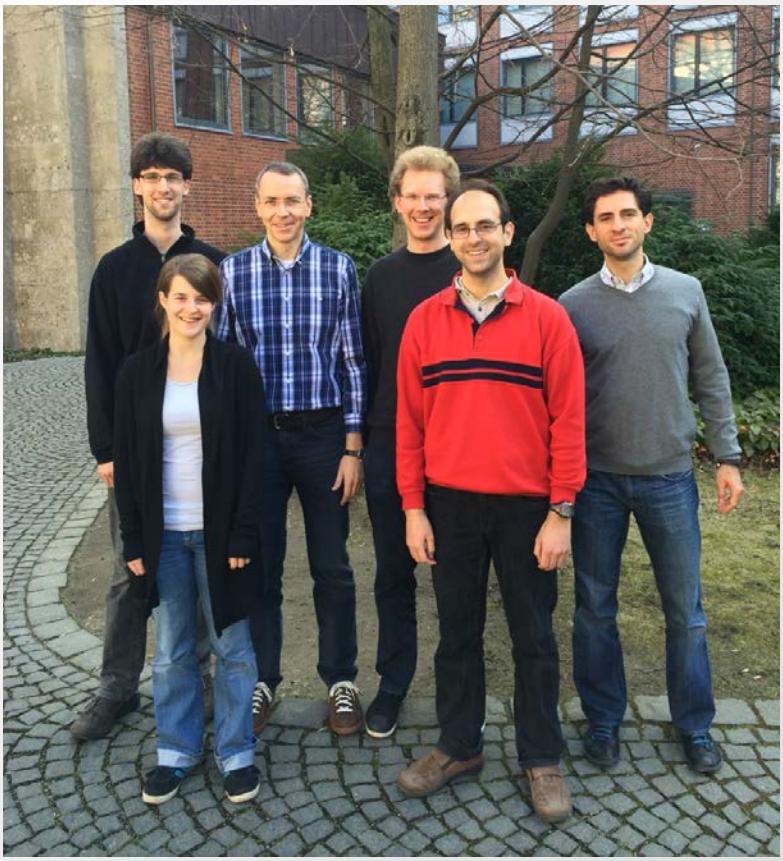

From left to right:

Christian Schweizer

Monika Aidelsburger

I.B.

Michael Lohse

Marcos Atala

Julio Barreiro

2D Berry Curvature Interferometer Team

Lucia Duca

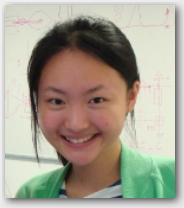

Tracy Li

Martin Reitter

Monika Schleier-Smith

IB

Ulrich Schneider

Sunday 22 June 14